

1 **Diurnal variations of NO₂ tropospheric vertical column density over the Seoul**
2 **Metropolitan Area from the Geostationary Environment Monitoring**
3 **Spectrometer (GEMS): seasonal differences and ~~the influence of~~ the influence of**
4 **~~impacts of varying the *aa priori* NO₂ profile, data~~**

서식 지정함: 글꼴: 기움임꼴 없음

5
6 Seunghwan Seo¹, Si-Wan Kim^{1,2*}, Kyoung-Min Kim¹, Andreas Richter³, Kezia Lange³,
7 John P. Burrows³, Junsung Park^{4**}, Hyunkee Hong⁵, Hanlim Lee⁴, Ukkyo Jeong⁴, Jung-
8 Hun Woo^{6***}, and Jhoon Kim^{1*}

9
10 ¹Department of Atmospheric Sciences, Yonsei University, Seoul, Republic of Korea

11 ²Irreversible Climate Change Research Center, Yonsei University, Seoul, Republic of
12 Korea

13 ³Institute of Environmental Physics, University of Bremen, Bremen, Germany

14 ⁴Division of Earth Environmental System Science, Major of Spatial Information
15 Engineering, Pukyong National University, Busan, Republic of Korea

16 ⁵National Institute of Environmental Research, Incheon, Republic of Korea

17 ⁶Department of Technology Fusion Engineering, College of Engineering, Konkuk
18 University, Seoul, Republic of Korea

19

20 *To whom correspondence should be addressed:

21 Si-Wan Kim (e-mail: siwan.kim@yonsei.ac.kr) and Jhoon Kim (e-mail:
22 jkim2@yonsei.ac.kr).

23 ***now at: Center for Astrophysics | Harvard & Smithsonian, Cambridge, MA, USA

- 1 ***now at: Graduate School of Environmental Studies, Seoul National University, Seoul,
- 2 Republic of Korea
- 3 Date: 10/13/2024
- 4

1 **Abstract**

2 The Geostationary Environment Monitoring Spectrometer (GEMS), launched in 2020,
3 provides both temporally and spatially continuous air quality data from geostationary
4 Earth orbit (GEO). This study first investigates the seasonal variations and diurnal
5 behavior patterns of nitrogen dioxide (NO₂) tropospheric vertical column densities
6 (TropVCDs) over the Seoul Metropolitan Area (SMA) using GEMS data, retrieved by
7 the IUP-UB algorithm. We found that both the magnitude of the amounts of NO₂
8 TropVCDs and ~~its~~ diurnal behavior patterns have significant seasonal
9 dependences early vary according to the seasons. In January, the highest NO₂
10 TropVCD values in the range of 27.5 – 28.9 × 10¹⁵ molec. cm⁻² during among the four
11 seasons were observed appear at 15:00 local time (LT), and NO₂ TropVCD with
12 increases from the first retrieved values at 10:00 LT continuously increasing diurnal
13 patterns. On the other hand, we find the lowest values (7.4 – 8.8 × 10¹⁵ molec. cm⁻²) are
14 found at ~14:00 LT in July. The VCD values in July are increasing until 10 LT,
15 diminishing until 14 LT, and then rebounding increased up to 10:00 LT, then decreased
16 until 14:00 LT, but then began to increase again after. These distinguishing different
17 diurnal behaviors of patterns the TropVCDs in the across different the seasons
18 reflect imply the differences in of photochemical and meteorological conditions as well
19 as the emissions of NO_x. Photochemical transformations are typically more, mostly
20 rapid active in July and slow er in January. We also investigated the role of horizontal
21 wind on the NO₂ TropVCDs. The absolute values and diurnal behavior patterns of NO₂
22 TropVCDs are significantly influenced by changed by setting different the wind speed
23 filter, except in July. MEspecially, moderate (wind speed ≥ 3m/s) or strong wind (wind
24 speed > 5m/s) reduced the magnitude of the makes diurnal behavior patterns in January
25 flattened, implying that indicating the NO₂ plumes were transported to the downwind
26 regions. Finally/Lastly, we investigate compared the retrieved NO₂ TropVCDs with that
27 retrieved using different various a priori NO₂ data simulated by from TM5 and WRF-
28 Chem, calculated using with the most recent latest emission inventories. Although
29 simulated VCDs from WRF-Chem and TM5 show differences/serapancies of up to a

서식 지정함: 아래 첨자

서식 지정함: 아래 첨자

서식 지정함: 아래 첨자

1 ~~factor 2.75-times~~, retrieved NO₂ TropVCDs using each *a priori* data have almost
2 identical values and ~~-~~diurnal ~~behaviors~~patterns, except in July. Notably, ~~the~~ diurnal
3 ~~behavior~~patterns of ~~the~~ retrieved NO₂ TropVCDs are independent ~~of with~~ those from
4 ~~the~~ two chemical transport models, indicating that observations of slant column
5 densities are the ~~dominant factor in-main~~ determining ~~theants-of~~ diurnal ~~behavior~~
6 ~~patterns~~ of NO₂ TropVCDs. Changes of ~~the~~ model horizontal resolution and ~~volatile~~
7 ~~organic compounds~~ (VOC) emission inventory do not affect ~~significantly the~~ retrieved
8 NO₂ TropVCDs in this study. However, when the *a priori* ~~NO₂~~ vertical profile was fixed
9 as the values at 13:45 LT, the diurnal patterns of NO₂ TropVCDs ~~show~~showed
10 ~~significant -meaningful~~ changes with differences of up to -18.3%.

서식 지정함: 아래 첨자

서식 지정함: 글꼴: 기울임꼴 없음

서식 지정함: 글꼴: 기울임꼴 없음, 아래 첨자

서식 지정함: 글꼴: 기울임꼴 없음

1 **1. Introduction**

2 Nitrogen dioxide (NO₂) is one of the most important trace gases— ~~involved in the~~
3 photochemical ~~mechanisms, which reactions~~ determine the tropospheric distributions
4 ~~of related to tropospheric ozone and secondary aerosol chemistry~~ (Milford et al., 1989).
5 ~~Beginning with the launch of the passive remote sensing instrument GOME on ESA~~
6 ~~ERS-2 (Burrows et al., 1999) in 1995, then followed by SCIAMACHY~~ ~~In recent~~
7 ~~decades, on ESA Envisat in 2002 (Burrows et al., 1995 and Bovensmann et al., 1999),~~
8 ~~OMI on NASA AURA (Levelt et al., 2004), GOME-2 on ESA EUMETSAT Metop A,~~
9 ~~B and C (Callies et al., 2000, Munro et al., 2016), and Trop~~ROPOMI on the ESA
10 Sentinel 5 Precursor in 2018 (Veeffkind et al., 2012), the amounts and distributions of
11 ~~stratospheric and environmental satellites such as GOME, OMI, SCIAMACHY, and~~
12 ~~TROPOMI have observed~~ tropospheric NO₂ vertical column densities (TropVCDs)
13 ~~have been retrieved at increasing spatial resolutions from these instruments, which all~~
14 ~~fly in sun-synchronous low earth orbit (LEO). By~~ ~~from space (Burrows et al., 1999,~~
15 ~~Levelt et al., 2006, Bovensmann et al., 1999, Veeffkind et al., 2012), which have been~~
16 ~~extensively~~ ~~Using the retrieved NO₂ TropVCDs from the LEO instruments, have the~~
17 ~~utilized for~~ tropospheric ~~detection of various nitrogen oxides oxide~~ sources ~~have been~~
18 ~~identified and their~~ NO_x emissions ~~have been estimated,~~ and the chemistry of the ~~t~~
19 ~~and probing~~ tropospheric ~~related chemistry~~ ~~has~~ been studied from the local to the
20 global scale ~~across the globe~~. While ~~instruments on board~~ ~~these low Earth orbit (LEO)~~
21 satellites provide spatially continuous data, observations are obtained only once or
22 twice per day. ~~It was recognized in the late 1990s that instruments similar to~~
23 ~~SCIAMACHY in geostationary orbit (GEO) would potentially deliver the diurnal~~
24 ~~variations of key trace gases (see the Geo~~TropeROPE concept in Burrows et al., 2004
25 ~~and references therein).~~ The measurements at the top of the atmosphere of the
26 Geostationary Environment Monitoring Spectrometer (GEMS), launched in 2020, ~~yield~~
27 ~~the first~~ ~~produces~~ not only spatially but also temporally continuous air quality data over
28 Asia from the geostationary ~~orbit~~ Earth-orbit (GEO) (~~see~~ ~~J.~~ Kim et al., 2020).

서식 지정함: 아래 첨자

1 Mathematical inversion of the GEMS observations provides diurnal variations
2 of the NO₂ TropVCD. These data products enable, ~~enabling the analysis of~~ seasonal
3 changes not only in pollutant concentration but also in temporal characteristics, such as
4 the times of the maxima and minima, ~~peak times~~ and the sources and sinks of
5 NO₂ processes of accumulation and loss, which vary by diurnally and seasonally, to be
6 studied for the first time from space.

서식 있음: 들여쓰기: 첫 줄: 1.41 cm

서식 지정함: 아래 첨자

7 As part of the differential optical absorption spectroscopy (DOAS) retrieval of
8 In the process of NO₂ TropVCD data retrieval, air mass factors (AMF) are used to
9 convert slant column density (SCD) to VCD. The assumptions used in the AMF
10 calculation are explained in ~~(Richter and Burrows (2002) and Palmer et al. (2001))~~.
11 In agreement with other studies, Lorente et al. (2017) reported that the AMF
12 calculation is the largest source of error or uncertainty in NO₂ satellite retrievals. This
13 is because of the assumption used to determine the, ~~especially with several ancillary~~
14 ancillary or prior data used in the AMF calculation, such as surface albedo, terrain
15 height, cloud parameters, and trace gas profiles. Consequently, ~~Therefore~~, selecting the
16 selection of optimal and appropriate a priori data is essential ~~necessary~~ to accurately
17 retrieve NO₂ TropVCDs from the observations of any nadir-sounding satellite
18 spectrometer observations. This is in addition to the need to separate upper atmospheric
19 NO₂ from that in the troposphere.

서식 지정함: 아래 첨자

서식 지정함: 아래 첨자

20 In this ~~This~~ study we investigate two important issues using the aspects of
21 GEMS NO₂ TropVCD data over the Seoul Metropolitan Area (SMA): (1) seasonal
22 variations and (2) the influence ~~impact~~ of a priori profiles on the retrieved GEMS NO₂
23 TropVCDs and (2) the seasonal variation of the GEMS NO₂ TropVCD. In section 2 we
24 describe the methods and data used.

서식 있음: 들여쓰기: 첫 줄: 1.41 cm

25 Prior to our geophysical interpretation of the NO₂ TropVCD, in ~~Section 3 we~~
26 compared three GEMS datasets, retrieved with different a priori data from the WRF-
27 Chem model. Thereby we investigated the influence of the inventories of the emissions

서식 지정함: 아래 첨자

서식 지정함: 글꼴: 기울임꼴

1 ~~of NO_x, defined as the sum of nitrogen monoxide (NO) and nitrogen dioxide (NO₂) in~~
2 ~~an air mass, on the simulated and retrieved NO₂ TropVCD.~~

서식 지정함: 아래 첨자

서식 지정함: 아래 첨자

3 In Section 4.3, we utilized two chemical transport models (CTM), ~~the~~ Weather
4 Research and Forecast model combined with Chemistry (WRF-Chem) and the global
5 chemistry transport model TM5 (Tracer Model 5) to analyze both ~~the~~ seasonal
6 variations and ~~the influence of a priori NO₂ profiles data impacts. The seasonal~~
7 ~~changes~~ ~~Changes~~ in the magnitudes ~~value~~ and the time of the maxima of the diurnal NO₂
8 TropVCD, which we define as the ~~s~~ and peak times, were investigated. ~~According to~~
9 ~~the seasons were analyzed. The d~~ Differences in the spatial distributions of NO₂
10 TropVCD between the WRF-Chem- and TM5-based GEMS datasets ~~using~~ ~~that~~
11 ~~utilized~~ different *a priori* data, were identified for each season and peak time. We also
12 ~~analyzed~~ ~~analyzed~~ the ~~influence of wind speed seasonal~~ ~~on the~~ variations in the
13 ~~magnitude values~~ and diurnal ~~behavior patterns~~ of the retrieved NO₂ TropVCDs, ~~based~~
14 ~~on wind speed. In Section 4, we compared three GEMS datasets retrieved with different~~
15 ~~a priori data from the WRF-Chem model. This study includes the impacts of both NO_x~~
16 ~~emission inventories and vertical distributions on NO₂ TropVCDs.~~

서식 지정함: 아래 첨자

서식 지정함: 아래 첨자

서식 지정함: 아래 첨자

서식 있음: 들여쓰기: 첫 줄: 1.41 cm

20 2. Data and methods

서식 있음: 표준

21 2.1. GEMS products

22 GEMS is an ultraviolet-visible (UV-VIS) instrument, ~~measuring contiguously the~~
23 ~~spectral range~~ ~~with the spectral coverage from~~ of 300 ~~to~~ 500 nm ~~at a spectral~~
24 ~~resolution of ~with~~ 0.6 nm ~~spectral resolution~~ (J. Kim et al., 2020). The nominal spatial
25 resolution is 3.5 km × 7.7 km for gases including NO₂ ~~data products~~. The overall field
26 of regard (FOR) of GEMS covers 75° – 145°E longitude and 5°S – 45°N latitude.

1 GEMS measures hourly during the daytime. The number of observations varies
2 depending on the month, ~~s~~ as a result of the length of the day and the measurement
3 strategy. For—for South Korea, observations are least frequent in January, with six
4 observations per day, and most frequent from April to September, with ten observations
5 per day. We utilized GEMS NO₂ TropVCD data with the IUP-UB algorithm (GEMS
6 IUP-UB products) in January, April, July, and October 2021 – detailed explanations of
7 GEMS IUP-UB products are shown in Section 2.1.1.

8

9 2.1.1. GEMS IUP-UB products v1.0

10 The GEMS NO₂ vertical columns used in this study are from the scientific data product
11 of the University of Bremen, version 1.0 (Lange et al., 2024, Richter et al., *in*
12 *preparation*). NO₂ slant columns are retrieved in the large fitting window 405 – 485nm
13 to reduce noise. In addition to the cross-sections of other absorbing species (O₃, O₄,
14 H₂O and liquid water) pseudo cross-sections for the Ring effect, for GEMS instrument
15 polarization sensitivity and the effects of scene inhomogeneity are included. The
16 stratospheric correction is performed using the STRatospheric Estimation Algorithm
17 from Mainz (STREAM) (Beirle et al., 2016). Conversion to vertical tropospheric
18 columns is based on look-up tables of altitude dependent air mass factors calculated
19 with the radiative transfer model SCIATRAN (Roazanov et al., 2014) using Lambertian
20 equivalent reflectivity (LER) surface reflection values from the TROPOMI climatology
21 (Tilstra et al., 2023). To apply the cloud correction, adjusted cloud fractions and
22 pressure from the GEMS L2 cloud product were ~~used~~adopted. Further information
23 about IUP-UB products is described in Richter et al. (*in preparation*). The NO₂ *a priori*
24 data ~~are different vary between~~ the different model simulations, which we call runs,
25 as ~~explained~~described below.

26

메모 포함[JP1]: This will probably have to be at least submitted to be referenced.

2.2. Experiment designs

To analyze the spatiotemporal characteristics of GEMS NO₂ VCDs and the impacts of different *a priori* data on the retrieved values, we ~~undertook~~ set five experiments, ~~called~~ – TM5, CTRL, CONST, FINE, and MIXED.

The TM5 ~~experiment~~ ~~ease~~ ~~applies~~ ~~utilizes~~ the standard GEMS IUP-UB products v1.0, which use ~~the~~ TM5 model, as their *a priori* data (Huijnen et al., 2010; Williams et al., 2017). The meteorological data for TM5 simulations are obtained from the European Centre for Medium-Range Weather Forecasts (ECMWF) operational forecast data. For the anthropogenic NO_x emission inventory of TM5, the MACCity emission estimates are adopted (Granier et al., 2011), which have no diurnal ~~variation~~ ~~changes~~ of NO_x emissions. The outputs from TM5 model have ~~at~~ the horizontal resolution of 1° × 1° and 34 vertical layers.

For the other four ~~numerical~~ ~~experiment~~ ~~eases~~ (CTRL, CONST, FINE, and MIXED), WRF-Chem version 4.4 was ~~used~~ ~~utilized~~ to generate *a priori* data (Grell et al., 2005; Skamarock et al., 2021). The chemistry scheme follows the Regional Atmospheric Chemistry Mechanism (RACM) with Secondary Organic Aerosol-Volatility Basis Set (SOA-VBS) option (chem_opt = 108) (Ahmadov et al., 2012). The horizontal resolution of WRF-Chem simulation is 28 km × 28 km, except for the FINE ~~ease~~ ~~run~~ (12 km × 12 km). All simulations have 59 customized vertical layers. To ~~account~~ ~~for~~ ~~every~~ the stratospheric vertical profiles, the Whole Atmosphere Community Climate Model (WACCM) model outputs were combined with the WRF-Chem data (ACOM/NCAR/UCAR, 2020, last access: 05 Dec 2022). The combined data comprises a total of 113 vertical layers. Detailed model configuration is described in Kim et al. (2023, 2024). For the anthropogenic emission inventories, the Air Quality in Northeast Asia (AQNEA) emission inventory version 2 was adopted. Since the reference year of AQNEA version 2 is 2019, the anthropogenic NO_x emissions decreased by 20% to ~~account for the~~ ~~consider~~ decreasing trends of NO_x emissions from 2019 to 2021. We

서식 있음: 들여쓰기: 첫 줄: 1.41 cm

1 applied the normalized diurnal variabilities of NO_x emissions obtained from the Los
2 Angeles Basin in Kim et al. (2016), but shifting the values by one hour (Figure 1). For
3 the CONST case, only the *a priori* profiles at 13:45 LT were used to retrieve the VCD
4 values. To investigate the impact of VOC emissions on the retrieved NO₂-VCDs, we
5 replaced the one hour earlier (Figure 1). For the CONST run, only the *a priori* profiles
6 at 13:45 LT were used to retrieve the NO₂ TropVCD. To investigate the impact on the
7 volatile organic compounds (VOC) emissions of the anthropogenic VOC emissions we
8 used by the KORUS emission inventory version 5 (Jang et al., 2020, Woo et al., 2012)
9 in the MIXED *eas*erun. We retrieved four months (January, April, July, and October
10 2021) for the TM5 and CTRL *eas*eruns, and one month (July 2021) for the other
11 *eas*eruns. The experimental designs are summarized in Table 1.

서식 지정함: 아래 첨자

서식 있음: 들여쓰기: 첫 줄: 1.41 cm

14 3. Spatiotemporal characteristics of GEMS NO₂-TropVCD

15 In this section, we analyze the spatiotemporal characteristics of GEMS NO₂-TropVCD
16 using the TM5 and CTRL cases on two aspects—seasonal variations and transport
17 impacts—over the SMA region (126.5—127.3°E, 37.2—37.8°N) in 2021.

19 3.1. Seasonal variations

20 Figure 2 displays diurnal patterns of retrieved and *a priori* NO₂-TropVCDs during
21 weekdays in January, April, July, and October 2021 over the SMA region from the TM5
22 and CTRL cases. The pixels with wind speed faster than 3m/s are excluded to remove
23 the impacts of transport. The impacts of transport on NO₂ columns are analyzed in
24 Section 3.2.

25 In January, NO₂-TropVCDs show continuous increases from 10 local time (LT)

서식 있음: 들여쓰기: 첫 줄: 1.41 cm

1 to 15 LT. During the wintertime, NO_2 in the urban region is accumulated because of
2 slow photochemical loss process due to the less solar radiation and low temperature.
3 The maximum values of retrieved TropVCDs in January are 27.5×10^{15} molec. cm^{-2}
4 (TM5) and 28.9 (CTRL) $\times 10^{15}$ molec. cm^{-2} at 15 LT, while the *a priori* NO_2 TropVCDs
5 show maximum values of 11.2×10^{15} molec. cm^{-2} (TM5) and 21.9×10^{15} molec. cm^{-2}
6 (CTRL) at the same time. Those higher values of retrieved VCDs compared to model
7 VCDs may be due to uncertainty of the bottom-up NO_x emissions in January and/or
8 dilution of plumes dependent on the model horizontal resolution. For other months,
9 VCDs show the peak values at the earlier time due to faster photochemistry than in
10 January. Figure 3 shows the diurnal variations of OH concentrations averaged across
11 boundary layer height in each month. The OH concentration in January is about an order
12 smaller than that in July. In April, NO_2 TropVCDs increased until 12 LT, and then
13 maintain similar levels until 17 LT. The maximum values occurred at 12 LT for the
14 CTRL case (21.4×10^{15} molec. cm^{-2}). The maximum retrieved values of the TM5 case
15 appeared at 17 LT (21.9×10^{15} molec. cm^{-2}). Although the retrieved VCDs from the
16 TM5 and CTRL cases have almost identical diurnal patterns until 15 LT, the clear
17 discrepancy of 1.6×10^{15} molec. cm^{-2} (8.1%) between the two cases can be found at 17
18 LT, when *a priori* VCD value sharply increased from the CTRL case. In July, both the
19 TM5 (12.2×10^{15} molec. cm^{-2}) and CTRL (13.9×10^{15} molec. cm^{-2}) cases show the
20 maximum values at 10 LT, that is the earliest time among the four months. After the
21 peak time, NO_2 VCDs are diminished by photochemical loss processes until 14 LT, and
22 then rebounded. In other seasons, the minimum values were observed in the morning;
23 however, in July, the minimum occurred at 14 LT. This unique pattern implies that
24 photochemical reactions are most rapid during summer, leading to more active chemical
25 removal processes compared to the emission levels (Figure 3). The two cases show
26 similar diurnal patterns, but the retrieved values of the CTRL case during 10—14 LT
27 are up to 2.1×10^{15} molec. cm^{-2} higher than those of the TM5 case. The diurnal change
28 of *a priori* VCDs from the CTRL case shows similar pattern with retrieved VCDs;

1 although the absolute values of *a priori* data are $3.9\text{--}8.2 \times 10^{15}$ molec. cm^{-2} higher
2 than those of retrieved data. On the other hand, the *a priori* data from the TM5 case
3 show continued decreases during 8–14 LT, reflecting diurnally varying photochemistry
4 with similar levels of NO_x emissions throughout the day. In October, there are broad
5 peaks from 12 LT to 15 LT. Overall diurnal patterns—increasing until 12 LT and
6 maintaining the levels of NO_2 VCDs after—are similar to those in April. The maximum
7 retrieved values are 25.1×10^{15} – 25.5×10^{15} molec. cm^{-2} for both the TM5 and CTRL
8 cases. As expected, the VCD values are the highest in January and lowest in July.

9 **Figure 4 and 5** display spatial distributions of retrieved NO_2 -TropVCDs in January,
10 April, July, and October 2021 from the TM5 and CTRL cases, respectively. In January,
11 a plume over the SMA region was developed as time passed. Also, the suburban areas
12 which surround the SMA region show relatively higher values (over 10×10^{15} molec.
13 cm^{-2}) compared to the other months. In April and October, the plumes over the SMA
14 are saturated until 12 LT and then diminished, but the values of surrounding regions are
15 maintained or even increased. In July, overall low values cover the SMA and nearby
16 regions for whole days. The maximum values appear at 10 LT, and then decreased until
17 14 LT. However, the NO_2 VCD rebounded at 16 LT. **Figure 6** displays the differences
18 between the TM5 and CTRL cases—red color indicates the CTRL case has higher
19 values than the TM5 case; blue means opposite. The CTRL case shows higher VCD
20 values than the TM5 case for all times in July. The largest differences over the SMA
21 region are found at 12 LT in July with differences of 2.1×10^{15} molec. cm^{-2} . In other
22 months, the CTRL case generally have higher values of VCD than the TM5 case over
23 the Seoul and urban regions, while there are lower values of VCD from the CTRL case
24 over rural regions.

26 **3.2. Impacts of horizontal transport**

27 **Figure 7** shows diurnal patterns of retrieved NO_2 -TropVCDs from the CTRL case with

1 different wind conditions. The black lines indicate calm cases (wind speed lower than
2 3m/s), the green line mean strong wind cases (wind speed faster than 5m/s), and the
3 blue lines are the average values with no wind filters. In January (Figure 7a), the diurnal
4 patterns of VCDs change largely as the wind conditions change. In the calm case (black
5 solid), VCD values steadily increased due to the slow chemical loss with high emissions
6 in this season. In windy cases, however, diurnal changes in the retrieved columns are
7 negligible. Although the chemical loss is slow during wintertime, the accumulation of
8 NO₂ was mitigated as strong winds transported high concentrations of NO₂ to
9 downwind regions. The differences between calm and other cases were most significant
10 at 15 LT, further indicating that continuous outflow due to transport suppressed the
11 accumulation. As the wind speed increased, there was a noticeable reduction in VCD
12 values, which indicates a clear inverse relationship between wind speed and VCDs. The
13 values of calm, average (blue solid), and strong wind (green solid) are 19.0—28.9, 17.2
14 —19.8, and 12.1—13.4 × 10¹⁵ molec. cm⁻², respectively. In April (Figure 7b) and
15 October (Figure 7d), the averaged values with no wind filters (blue solid) have different
16 diurnal patterns, but the peak times appear almost simultaneously with the calm case.
17 In July (Figure 7c), however, the diurnal patterns from the calm case and no wind filters
18 are nearly identical, implying that the wind speeds are overall slow in July. In summary,
19 the transport effect is maximized in wintertime, changing not only the absolute values
20 but also diurnal patterns of VCDs—considerate handling of transport effects is required
21 for analyzing NO₂-TropVCDs and estimations of top-down NO_x emissions. The role of
22 transport still needs to be considered even though the wind speed is relatively slow
23 during summertime (Yang et al., 2024).

24 25 **3.4. Impacts of different *a priori* data on the retrieved NO₂ TropVCDs**

26 As shown in Section 3, the retrieved NO₂-TropVCDs can be changed by using different
27 *a priori* data, although the same retrieval algorithm was utilized. We In this section, we

1 compared retrieved NO₂ TropVCDs from the five different simulations, or easesruns, to
2 studyanalyze the impacts of *a priori* data used in AMF calculations on the retrieved ed
3 NO₂ TropVCDvals. We also investigated the vertical structures of NO₂ from each a
4 priori data.

서식 지정함: 아래 첨자

6 **34.1. Comparison between the CTRL and TM5 easesruns**

7 Retrieved NO₂ TropVCDs from the CTRL and TM5 easesruns exhibit similar diurnal
8 patterns, which are independent of the diurnal patterns of shown by their respective *a*
9 *priori* data (**Figure 2**). This suggests that the observed slant column density (SCD)
10 plays a more decisive role in the diurnal pattern of TropVCD than the influence of -a
11 priori used to determine the AMFdata. Nevertheless, differences in NO₂ TropVCDs
12 between the two easesruns were frequently observed, and arewith particularly noticeable
13 differences in July.

서식 있음: 들여쓰기: 첫 줄: 0 cm

서식 지정함: 글꼴: 굵게

14 **Figure 38** displays spatial distributions of AMF differences between the CTRL
15 and TM5 easesruns in January, April, July, and October 2021. In urban areas, the AMF
16 in the CTRL easesrun was generally lower (blue) than in the TM5 easesrun, but higher
17 values (red) were observed in the northern and eastern regions of Seoul. As a result, the
18 average values across the SMA domain were similar between CTRL and TM5 – the
19 diurnal patterns of averaged air mass factor over the SMA are shown in **Figure 49**. In
20 July, however, lower values in the CTRL easesrun were observed throughout Seoul and
21 its surrounding areas, leading to lower average AMF values for the SMA region during
22 most of the day. As a result, the TropVCD values in July were higher in the CTRL
23 easesrun (Figure 2c).

서식 있음: 들여쓰기: 첫 줄: 1.41 cm

24 In **Figure 540**, we compare NO₂ vertical profiles at 08, 10, 12, 14, and 16 LT
25 from the CTRL and TM5 easesruns. NO₂ values in the lower atmosphere in the CTRL
26 easesrun are much higher than those in the TM5 easesrun in July, which leads to lower

서식 지정함: 글꼴: 굵게

1 AMF ~~and thus~~ (higher NO₂ TropVCD columns).

서식 있음: 들여쓰기: 첫 줄: 1.41 cm

2 3 4 34.2. Comparisons between the CTRL and CONST, FINE, and MIXED ~~easerun~~s

5 ~~In Figure 6.11 the plots show~~ the diurnal patterns of retrieved and *a priori* NO₂ TropVCDs
6 in July 2021 over the SMA region from the CTRL ~~easerun~~ and the CONST, FINE, and
7 MIXED ~~easerun~~s. ~~are shown~~. Despite some changes in model resolution and VOC
8 emissions, the FINE and MIXED ~~easerun~~s did not show significant differences
9 compared to the CTRL ~~easerun~~. In particular, the MIXED ~~easerun~~ ~~resulted in almost~~
10 ~~almost~~ no difference in the *a priori* TropVCD values, resulting in nearly identical
11 retrieved NO₂ TropVCD values.

서식 지정함: 글꼴: 굵게 없음

서식 지정함: 글꼴: 굵게 없음

서식 지정함: 아래 첨자

12 On the other hand, the CONST ~~easerun~~, which used only the *a priori* vertical
13 profile ~~from~~ 13:45 LT in the retrieval process, exhibited clear differences ~~to from~~ the
14 CTRL ~~easerun~~. ~~Specifically it had~~ ~~it showed~~ lower values than the CTRL ~~easerun~~ before
15 ~~14:00~~ LT, but higher values after ~~14~~ LT. These differences ~~are can be~~ explained by
16 comparisons of vertical profiles from each ~~easerun~~s, which are displayed in **Figure 7.12**.
17 The vertical profile ~~shapes~~ of the CTRL, FINE, and MIXED ~~easerun~~s are identical,
18 indicating that AMF of each ~~easerun~~s have similar values. On the other hand, clear
19 differences of vertical profile ~~shape~~ ~~are apparent~~ ~~can be found~~ between the CTRL and
20 CONST ~~easerun~~s. Before 14:00 LT, the CTRL ~~easerun~~ showed lower sensitivity in the
21 upper layers ~~compared to the CONST easerun~~. ~~This~~ ~~resulting in~~ ~~indicates~~ a smaller
22 AMF and thus higher VCD values. In contrast, after 14:00 LT, the CTRL ~~easerun~~
23 exhibited higher sensitivity ~~to~~ NO₂ in the upper layers of the troposphere, leading to
24 a larger AMF and consequently lower VCD values compared to the CONST ~~easerun~~.
25 These differences in the vertical profile arise from ~~effects~~ ~~factors~~ such as the
26 development of the mixing layer and variations in emissions throughout the day. ~~This~~

서식 지정함: 아래 첨자

1 ~~implies that, indicating that~~ providing optimal time-dependent ~~varying~~ *a priori* data for
2 the AMF calculation ~~plays a crucial role in shaping the diurnal pattern~~ will improve the
3 accuracy of ~~of~~ the retrieved NO₂ TropVCD.

서식 지정함: 아래 첨자

서식 있음: 들여쓰기: 첫 줄: 1.41 cm

4. Spatiotemporal characteristics of GEMS NO₂ TropVCD

6 We report on our investigation of the spatiotemporal characteristics of GEMS NO₂
7 TropVCD. We use the retrieved NO₂ TropVCD and those simulated by the TM5 and
8 CTRL runs to assess two geophysically important influences on the NO₂ TropVCD the
9 SMA region (126.5 – 127.3°E, 37.2 – 37.8°N) in 2021: –(1) the identification,
10 quantification and origin of the seasonal changes; and- (2) advection and convection of
11 air masses.

서식 지정함: 아래 첨자

서식 지정함: 아래 첨자

서식 지정함: 글꼴: 굵게 없음

4.1. Seasonal variations

13 Figure 2 displays diurnal patterns of retrieved and *a priori* NO₂ TropVCDs during
14 weekdays in January, April, July, and October 2021 over the SMA region from the TM5
15 and CTRL runs. The scenes with wind speed faster than 3m/s are excluded to remove
16 the transport impacts. The effects of transport on NO₂ columns are analyzed in Section
17 4.2.

18 In January, NO₂ TropVCDs continuously increase from 10:00 local time (LT)
19 to 15:00 LT. During the winter, NO₂ in the urban region accumulates
20 particularly in ~~particular~~ the boundary layer. Qualitatively, this is explained as follows.

서식 있음: 들여쓰기: 왼쪽: 0 cm, 첫 줄: 1.41 cm

21 As tropospheric solar UV radiation is low in winter and the atmosphere is cold,
22 photolysis frequencies are small. Similarly, ~~the low temperature results in the~~ rate
23 coefficients of many reactions are smaller at the lower winter temperatures compared
24 to those of the other seasons. In winter, the relatively slow loss of NO_x occurs through

서식 있음: 들여쓰기: 첫 줄: 1.41 cm, 탭: 13.47 글자(없음)

서식 있음: 들여쓰기: 왼쪽: 0 cm, 첫 줄: 1.41 cm

1 the three body reaction of hydroxyl (OH) with NO₂ to form nitric acid (HNO₃): Similarly,
 2 the low temperature result in the rate coefficients of many reactions are smaller at the
 3 lower winter temperatures compared to those of the other seasons. of the relatively
 4 slow loss of NO_x loss e.g. through the three body reaction of hydroxyl (OH) with NO₂
 5 to form nitric acid (HNO₃)



7 The smaller photolysis frequencies of reactions following photoexcitation in the
 8 reactions:



11 lead to slower production of i) the first excited state of oxygen (O({}^1D)) from the
 12 photolysis of ozone (O₃), ii) the hydroxyl radical (OH), and iii) the production of
 13 organic peroxy radicals (RO₂), and hydroperoxy (HO₂) through the oxidation of
 14 methane (CH₄) and volatile organic compounds (VOC) VOC. Some of the following
 15 reactions are involved:



- 서식 지정함: 아래 첨자
- 서식 지정함: 아래 첨자
- 서식 있음: 들여쓰기: 왼쪽: 1.41 cm, 첫 줄: 0 cm
- 서식 지정함: 아래 첨자
- 서식 지정함: 아래 첨자
- 서식 지정함: 위 첨자
- 서식 지정함: 아래 첨자
- 서식 지정함: 위 첨자
- 서식 지정함: 아래 첨자
- 서식 지정함: 아래 첨자
- 서식 지정함: 아래 첨자
- 서식 지정함: 아래 첨자
- 서식 지정함: 아래 첨자
- 서식 지정함: 글꼴: Times New Roman
- 서식 지정함: 글꼴: Times New Roman, 아래 첨자
- 서식 지정함: 글꼴: Times New Roman
- 서식 지정함: 위 첨자
- 서식 지정함: 아래 첨자
- 서식 지정함: 글꼴: Times New Roman
- 서식 지정함: 아래 첨자
- 서식 지정함: 위 첨자
- 서식 지정함: 아래 첨자
- 서식 지정함: 글꼴: Times New Roman
- 서식 지정함: 아래 첨자
- 서식 지정함: 글꼴: Times New Roman
- 서식 지정함: 글꼴: Times New Roman, 아래 첨자
- 서식 지정함: 글꼴: Times New Roman
- 서식 지정함: 글꼴: Times New Roman, 아래 첨자
- 서식 지정함: 글꼴: Times New Roman, 아래 첨자
- 서식 지정함: 글꼴: Times New Roman
- 서식 지정함: 글꼴: Times New Roman, 아래 첨자
- 서식 지정함: 글꼴: Times New Roman
- 서식 지정함: 글꼴: Times New Roman, 아래 첨자
- 서식 지정함: 글꼴: Times New Roman



6
7 Overall at low solar insolation, the low levels of actinic radiation result in
8 smaller amounts of OH and HO₂. The oxidation process is slow and HO₂ and OH
9 chemistry are coupled with NO_x chemistry and controlled by rate of oxidation of VOC
10 and CH₄ and the rate of HO₂ to OH through the rate of reaction (14) and the rate of loss
11 of HO₂ and NO_x for example through reaction (1).

12 In January the maximum values of retrieved TropVCDs in January are 27.5 ×
13 10¹⁵ molec. cm⁻² (TM5) and 28.9 × 10¹⁵ molec. cm⁻² (CTRL) at 15:00 LT, whereas
14 the a priori NO₂ TropVCDs have maxima of 11.2 × 10¹⁵ molec. cm⁻² (TM5) and 21.9
15 × 10¹⁵ molec. cm⁻² (CTRL) at the same time. These higher values of retrieved NO₂
16 TropVCDs relative to the model NO₂ TropVCDs are explained by the following
17 inadequate knowledge of the bottom-up diurnal NO_x emissions in January and/or the
18 dilution during the transport of plumes, which is dependent on the model horizontal
19 resolution.

20 For other months, the maxima of NO₂ TropVCDs occur at earlier times of the
21 day viz. in April at 12:00 (LT), in July at 10:00 (LT) and in October at 11:00 (LT). There
22 is also a second maximum at 15:00 (LT) in October. —The behavior of NO₂ TropVCD
23 in April, July and October, when compared to that in January, is explained by the

서식 지정함: 아래 첨자

서식 지정함: 아래 첨자

서식 지정함: 글꼴: Times New Roman

서식 지정함: 아래 첨자

서식 있음: 들여쓰기: 왼쪽: 1.4 cm

서식 지정함: 글꼴: Times New Roman

서식 지정함: 아래 첨자

서식 지정함: 글꼴: Times New Roman

서식 지정함: 아래 첨자

서식 지정함: 글꼴: Times New Roman

서식 지정함: 글꼴: Times New Roman, 아래 첨자

서식 지정함: 아래 첨자

서식 지정함: 글꼴: Times New Roman

서식 지정함: 글꼴: Times New Roman, 아래 첨자

서식 지정함: 아래 첨자

서식 지정함: 위 첨자/아래 첨자없음

서식 지정함: 아래 첨자

서식 지정함: 글꼴: Times New Roman

서식 지정함: 글꼴: Times New Roman, 아래 첨자

서식 지정함: 글꼴: Times New Roman

서식 지정함: 글꼴: Times New Roman, 위 첨자/아래 첨자없음

서식 있음: 들여쓰기: 첫 줄: 1.41 cm

서식 지정함: 아래 첨자

서식 지정함: 아래 첨자

서식 지정함: 아래 첨자

서식 지정함: 아래 첨자

서식 지정함: 아래 첨자

서식 있음: 들여쓰기: 첫 줄: 1.41 cm

1 following effects: i) faster tropospheric photolysis frequencies, as a result of higher
2 levels of tropospheric solar insolation and actinic radiation accelerating the
3 photochemical oxidation of CH₄ and VOC in April, July and October compared to
4 January; ii) generally faster reaction rate coefficients of the free radical reactions at the
5 higher temperatures, the rate coefficient of reaction (4) being an exception; -iii) the
6 different diurnal emissions of NO_x compared to those in January.

서식 지정함: 아래 첨자

7 **Figure 8** shows the diurnal variations of OH concentrations averaged across
8 boundary layer height in each month, calculated by the CTRL model run. The OH
9 concentration in January is about an order of magnitude smaller than that in July.

서식 지정함: 글꼴: 굵게

10 In April, NO₂ TropVCDs increased until 12:00 LT. It then maintains similar
11 levels until 17:00 -LT-. The maximum NO₂ TropVCD occurred at 12:00 LT for the
12 CTRL run (21.4×10^{15} molec. cm⁻²). The maximum NO₂ TropVCD for the TM5 run
13 appeared at 17:00 -LT-, being 21.9×10^{15} molec. cm⁻². However, the retrieved NO₂
14 TropVCDs from the TM5 and CTRL runs have almost identical behavior up to 15:00
15 LT. There is a difference of 1.6×10^{15} molec. cm⁻² (8.1%) between the two runs at 17:00
16 LT, when *a priori* NO₂ TropVCD value sharply increased from the CTRL run.

서식 지정함: 아래 첨자

17 In July, both the TM5 (12.2×10^{15} molec. cm⁻²) and CTRL (13.9×10^{15} molec.
18 cm⁻²) runs show maxima at 10:00 LT, i.e. the earliest for the four months investigated.
19 After the peak, NO₂ TropVCDs decrease, most likely due to more rapid photochemical
20 loss processes e.g. reaction (1) -until 14:00 LT, and then increase. In other seasons, the
21 minimum values were observed in the morning. However, in July, the minimum
22 occurred at 14:00 LT. This unique pattern of behavior is explained by the more rapid
23 photochemical production and removal reactions in summer. We infer that the chemical
24 removal becomes relatively more rapid than the emission and production of NO₂ (see
25 Figure 8). The two types of run show similar diurnal behavior, but the retrieved NO₂
26 TropVCD of the CTRL runs between 10:00 and 14:00 LT rise to 2.1×10^{15} molec. cm⁻²
27 i.e. higher than those of the TM5 runs. The diurnal change of *a priori* NO₂ TropVCD

서식 지정함: 아래 첨자

서식 지정함: 아래 첨자

1 EDs from the CTRL runs shows a similar behavior to that of the retrieved NO₂
2 TropVCDs, despite the magnitude of a priori NO₂ TropVCD being $3.9 - 8.2 \times 10^{15}$
3 molec. cm⁻² higher than those retrieved. On the other hand, the a priori NO₂ TropVCD
4 from the TM5 runs decreases between 08:00 and 14:00 LT, reflecting diurnally varying
5 photochemistry with similar levels of NO_x emissions throughout the day.

서식 지정함: 아래 첨자

6 In October, there are broad maxima of NO₂ TropVCD between 12:00 LT and
7 15:00 LT. Overall diurnal behavior comprises increases up to 12:00 LT, followed by
8 broad maxima, after which the NO₂ TropVCD are similar to those in April.

9 The highest retrieved values are in the range 25.1×10^{15} to 25.5×10^{15} molec.
10 cm⁻² for both the TM5 and CTRL runs. As expected, the NO₂ TropVCD are the highest
11 in January and lowest in July.

12 Figures 9 and 10 show the spatial distributions of retrieved NO₂ TropVCDs in
13 January, April, July, and October 2021 from the TM5 and CTRL runs, respectively. In
14 January, a plume over the SMA region developed as a function of time. Consequently,
15 the suburban areas, which surround the SMA region, experience relatively high NO₂
16 TropVCD ($> 10 \times 10^{15}$ molec. cm⁻²) compared to that retrieved in the other months. In
17 April and October, the plumes over the SMA are saturated prior to 12:00 LT and then
18 decrease. In contrast, the NO₂ TropVCD of the surrounding regions are relatively
19 constant or even increase. In July, the overall low values cover the SMA and nearby
20 regions for whole days. The maximum values appear at 10 LT, and then decreased until
21 14 LT. However, the NO₂ VCD rebounded at 16 LT. Figure 11 displays the differences
22 between the TM5 and CTRL runs – red color indicates the CTRL run has higher values
23 than the TM5 run; blue means opposite. The CTRL run shows higher VCD values than
24 the TM5 run for all times in July. The largest differences over the SMA region are found
25 at 12 LT in July with differences of 2.1×10^{15} molec. cm⁻². In other months, the CTRL
26 run generally have higher values of VCD than the TM5 run over the Seoul and urban
27 regions, while there are lower values of VCD from the CTRL run over rural regions.

서식 있음: 들여쓰기: 첫 줄: 1.41 cm

서식 지정함: 아래 첨자

서식 지정함: 아래 첨자

1
2
3
4
5
6
7
8
9
10
11
12
13
14
15
16
17
18
19
20
21
22
23
24
25
26

4.2. Impacts of horizontal transport

Figure 12 shows the diurnal behavior of the retrieved NO₂ TropVCDs from the CTRL run for different wind conditions. The black lines indicate calm runs (wind speed lower than 3m/s), the green line are a strong-wind runs (wind speed faster than 5m/s), and the blue lines are the average values with no wind filters. In January (Figure 12a), the diurnal behavior of the NO₂ TropVCDs change significantly with the wind conditions. In the calm run (black solid), NO₂ TropVCD steadily increases due to a combination of the emissions increasing and the slow chemical loss in this month. In windy runs, however, diurnal changes in the retrieved NO₂ TropVCD are negligible.

Although the chemical loss is slow during wintertime, the accumulation of NO₂ was mitigated as strong winds transported large concentrations of NO₂ to downwind regions. The differences between calm and other runs were most significant at 15:00 LT, further indicating that continuous outflow due to transport suppressed the accumulation. As the wind speed increased, there was a noticeable reduction in NO₂ TropVCD values, which indicates a clear inverse relationship between wind speed and VCDs, as shown in Edwards et al. (2024)s. The values of calm, average (blue solid), and strong wind (green solid) are 19.0 – 28.9, 17.2 – 19.8, and 12.1 – 13.4 × 10¹⁵ molec. cm⁻², respectively.

In April (Figure 12b) and October (Figure 12d), the averaged values with no wind filters (blue solid) have different diurnal behavior, but the maximum NO₂ TropVCD appear almost simultaneously with that of the calm low wind speed run. In July (Figure 7c), however, the diurnal behavior from the calm run and no wind filters are nearly identical, implying that the wind speeds are overall slow in July.

In summary, the transport effect is maximized in wintertime, changing not only the absolute values but also diurnal behavior of NO₂ Trop VCDs. Consequently,

서식 지정함: 아래 첨자

서식 지정함: 아래 첨자

서식 지정함: 아래 첨자

서식 지정함: 아래 첨자

메모 포함[JP2]: Please analysis for the influence of wind in April July and October i.e. create and plot green lines for these months.

서식 지정함: 아래 첨자

서식 지정함: 아래 첨자

1 transport must be taken into account when analyzing NO₂ TropVCDs and when
2 estimating top-down NO_x emissions. The role of transport needs to be taken into
3 account even for cases, where the wind speed is relatively slow during summertime
4 (Yang et al., 2024).

6 5. Conclusions

7 In this study, we analyzed the seasonal variations and diurnal ~~behavior pattern~~
8 ~~differences~~ of the retrieved GEMS IUP-UB NO₂ TropVCD, using the monthly mean
9 data in January, April, July and October. ~~The~~ effects of wind speed, and the impact
10 of *a priori* NO₂ profiles on the retrieval. Both in the CTRL and TM5 ~~cases~~, the
11 GEMS NO₂ product showed significant changes in quantity, diurnal pattern, and peak
12 time as the seasons changed. In winter, the values were the highest, with a gradual
13 increase over time, whereas in summer, the values were the lowest, reaching a minimum
14 in the afternoon. This is consistent with previous studies, which have shown that
15 atmospheric chemical reactions are more active in summer. Furthermore, we confirmed
16 that wind-driven transport significantly influences the diurnal patterns, clearly
17 demonstrating that advection and possibly convection need to be taken into account
18 when wind transport plays a crucial role in estimating top-down NO_x emissions are
19 estimated from an urban agglomeration such as SMA.

20 On the other hand, when using different *a priori* data to calculate VCD values,
21 more complex results emerged. A comparison between the CTRL and TM5 ~~cases~~
22 revealed that, despite different spatial resolution and emission characteristics, the
23 retrieved NO₂ TropVCDs exhibited similar diurnal patterns, with significant differences
24 only in July. Additionally, we found that the retrieved NO₂ TropVCDs had diurnal
25 ~~behaviors patterns~~ independent of the *a priori* data in both ~~cases~~. We infer,
26 suggesting that the observed SCD has a stronger ~~more decisive~~ influence on the
27 retrieved diurnal patterns than *a priori* profiles. Adjusting the horizontal resolution of

서식 지정함: 글꼴: (한글) + 본문 한글(맑은 고딕), 굵게 없음, 글꼴 색: 자동

서식 있음: 들여쓰기: 첫 줄: 1.41 cm, 단어 잘림 허용

메모 포함[P3]:

서식 있음: 들여쓰기: 첫 줄: 1.41 cm

서식 지정함: 아래 첨자

서식 지정함: 아래 첨자

1 the model (FINE easerun) or changing the VOC emissions data (MIXED easerun) also
2 resulted in no significant differences. However, in the CONST easerun, where only the
3 vertical profile at 14:00 LT was used in the retrieval process throughout the day, there
4 were significant differences in both the NO₂ Trop VCD values and diurnal patterns.
5 This reaffirms that the vertical shape factor of *a priori* data plays a critical role in NO₂
6 TropVCD retrievals.

서식 지정함: 아래 첨자

서식 지정함: 아래 첨자

7 Additionally, given that vertical as well as horizontal model resolution can
8 influence retrievals (Liu et al., 20132020), future studies should analyze the results
9 when the vertical resolution is adjusted. Furthermore, as highlighted by previous
10 studies, such as Lorente et al. (2017) and Hong et al. (2017), which emphasized the
11 importance of cloud parameters, aerosol characteristics, and surface albedo,
12 uncertainties arising from factors in addition to the~~beyond~~ *a priori* NO₂ profile ~~data~~
13 should further be investigated ~~also be considered~~ in the retrieval of NO₂ TropVCD
14 ~~satellite retrieval~~for both diurnal GEO observation and those ~~for~~om LEO. ~~process~~.

서식 있음: 들여쓰기: 첫 줄: 1.41 cm

서식 지정함: 아래 첨자

16 Data availability

17 GEMS measurement data retrieved by the IUP algorithm are available on request from
18 Andreas Richter (richter@iup.physik.uni-bremen.de). WRF-Chem v4.4 is available in
19 GitHub (wrf-model, 2022).

21 Author contributions

22 SWK initiated this study and secured funding. SS and SWK analyzed the satellite and
23 model data. SS, KMK, and SWK conducted the model simulations. AR, KL, and JPB
24 provided GEMS IUP products and analyzed the data. JK, JP, HH, HL, UJ retrieved and
25 analyzed the GEMS observations and discussed the results. JHW provided AQNEA
26 version 2 emission inventory. SS and SWK wrote the paper, with contributions from all

1 co-authors.

2

3 **Competing interests**

4 At least one of the authors is a member of the editorial board of Atmospheric
5 Measurement Techniques.

6

7 **Acknowledgement**

8 This work was supported by the National Research Foundation of Korea (NRF) grant
9 funded by the Korea government (MSIT) (No. 2020R1A2C2014131). All the
10 computing resources are provided by National Center for Meteorological
11 Supercomputer. Th contributions from the University of Bremen were supported by the
12 State and University of Bremen and the DLR.

13

14 **References**

15 Ahmadov, R., McKeen, S. A., Robinson, A. L., Bahreini, R., Middlebrook, A. M., de
16 Gouw, J. A., Meagher, J., Hsie, E.-Y., Edgerton, E., Shaw, S., and Trainer, M.: A
17 volatility basis set model for summertime secondary organic aerosols over the eastern
18 United States in 2006, *J. Geophys. Res. Atmos.*, 117, D06301,
19 <https://doi.org/10.1029/2011JD016831>, 2012.

20 Atmospheric Chemistry Observations & Modeling/National Center for Atmospheric
21 Research/University Corporation for Atmospheric Research: Whole Atmosphere
22 Community Climate Model (WACCM) Model Output, Research Data Archive at the
23 National Center for Atmospheric Research, Computational and Information System
24 Laboratory, <https://doi.org/10.5065/G643-Z138>, (last access: 05 December 2022),
25 2020.

메모 포함[JP4]: Andreas please DLR project and any
ESA numbers

1 Beirle, S., Hörmann, C., Jöckel, P., Liu, S., Penning De Vries, M., Pozzer, A., Sihler, H.,
2 Valks, P. and Wagner, T.: The STRatospheric Estimation Algorithm from Mainz
3 (STREAM): Estimating stratospheric NO₂ from nadir-viewing satellites by weighted
4 convolution, *Atmos. Meas. Tech.*, 9(7), 2753–2779, doi:10.5194/amt-9-2753-2016,
5 2016.

6 ~~Boersma, K. F., Eskes, H. J. and Brinksma, E. J.: Error analysis for tropospheric NO₂~~
7 ~~retrieval from space, *J. Geophys. Res. Atmos.*, 109(4), doi:10.1029/2003jd003962,~~
8 ~~2004.~~

9 Bovensmann, H., Burrows, J. P., Buchwitz, M., Frerick, J., Noël, S., Rozanov, V. V.,
10 Chance, K. V., and Goded, A. P. H.: SCIAMACHY: Mission Objectives and
11 Measurement Modes, *J. Atmos. Sci.*, 56, 127-150, [https://doi.org/10.1175/1520-](https://doi.org/10.1175/1520-0469(1999)056<0127:SMOAMM>2.0.CO;2)
12 [0469\(1999\)056<0127:SMOAMM>2.0.CO;2](https://doi.org/10.1175/1520-0469(1999)056<0127:SMOAMM>2.0.CO;2), 1999.

13 ~~Buchholz, R. R., Emmons, L. K., Tilmes, S., and The CESM2 Development Team:~~
14 ~~CESM2.1/CAM Chem Instantaneous Output for Boundary Conditions,~~
15 ~~UCAR/NCAR Atmospheric Chemistry Observations and Modeling Laboratory,~~
16 ~~Lat: 5 to 45, Lon: 75 to 145, 28 Nov 2022, <https://doi.org/10.5065/NMP7-EP60>,~~
17 ~~2019.~~

18 ~~61) Burrows J. P., Hölzle E., Goede A. P. H., Visser H. and Fricke, W., 1995, ":~~
19 ~~SCIAMACHY - Scanning Imaging Absorption Spectrometer for Atmospheric~~
20 ~~Chartography", *ACTA ASTRONAUTICA Astronautica* Volume: 35 Issue: 7 Pages:~~
21 ~~445-451 Published: APR 1995 DOI10.1016/0094-5765(94)00278-T, 35, 445-461,~~
22 ~~[https://doi.org/10.1016/0094-5765\(94\)00278-T](https://doi.org/10.1016/0094-5765(94)00278-T), 1995.~~

23 Burrows, J. P., Weber, M., Buchwitz, M., Rozanov, V., Ladstätter-Weissenmayer, A.,
24 Richter, A., DeBeek, R., Hoogen, R., Bramstedt, K., Eichmann, K.-U., Elsinger, M.,
25 and Perner, D.: The Global Ozone Monitoring Experiment (GOME): Mission
26 Concept and First Scientific Results, *J. Atmos. Sci.*, 56, 151-175,

서식 지정함: 글꼴: 기울임꼴

서식 지정함: 글꼴: 기울임꼴

1 [https://doi.org/10.1175/1520-0469\(1999\)056<0151:TGOMEG>2.0.CO;2](https://doi.org/10.1175/1520-0469(1999)056<0151:TGOMEG>2.0.CO;2), 1999.

2 [Burrows, J. P., Bovensmann, H., Bergametti, G., Flaud, J. M., Orphal, J., Noël, S.,](#)
3 [Monks, P. S., Corlett, G. K., Goede, A. P. H., von Clarmann, T., Steck, T., Fischer,](#)
4 [H., and Friedl-Vallon, F., 2002, “: The geostationary tropospheric pollution explorer](#)
5 [\(GeoTROPE\) missions: objects, requirements and mission concept”](#), [Source: Trace](#)
6 [Constituents in the Troposphere and Lower Stratosphere: Book Series: Editor\(s\):](#)
7 [Burrows J. P., Thompson A. M.: *Advances in Space Research*, Volume: 34 Issue: 4](#)
8 [Special Issue: Sp. Iss., 2004 Pages: 682-687Published: 2004 34, 682-687,](#)
9 <https://doi.org/10.1016/j.asr.2003.08.067>, 2004.

10 [Callies, J., Corpaccioli, E., Eisinger, M., Hahne, A., and Lefebvre, A.: GOME-2-](#)
11 [Metop's second-generation sensor for operational ozone monitoring, *ESA Bulletin*,](#)
12 [102, 28–36, 2000.](#)

13 Edwards, D. P., Martínez-Alonso, S., Jo, D.-S., Ortega, I., Emmons, L. K., Orlando, J.
14 J., Worden, H. M., Kim, J., Lee, H., Park, J., and Hong, H.: Quantifying the diurnal
15 variation of atmospheric NO₂ from observations of the Geostationary Environment
16 Monitoring Spectrometer (GEMS), *Atmos. Chem. Phys.*, 24, 8943-8961,
17 <https://doi.org/10.5194/acp-24-8943-2024>, 2024.

18 [Emmons, L. K., Walters, S., Hess, P. G., Lamarque, J. F., Pfister, G. G., Fillmore, D.,](#)
19 [Granier, C., Guenther, A., Kinnison, D., Laepple, T., Orlando, J., Tie, X., Tyndall, G.,](#)
20 [Weidinyer, C., Baugheum, S. L., and Kloster, S.: Description and evaluation of the](#)
21 [Model for Ozone and Related chemical Tracers, version 4 \(MOZART 4\), *Geosci.*](#)
22 [Model Dev.](#), 3, 43–67, <https://doi.org/10.5194/gmd-3-43-2010>, 2010.

23 [Emmons, L. K., Schwantes, R. H., Orlando, J. J., Tyndall, G., Kinnison, D., Lamarque,](#)
24 [J. F., Marsh, D., Mills, M. J., Tilmes, S., Bardeen, C., Buchholz, R. R., Conley, A.,](#)
25 [Gettelman, A., Garcia, R., Simpson, I., Blake, D. R., Meinardi, S., and Pétron, G.:](#)
26 [The Chemistry Mechanism in the Community Earth System Model Version 2](#)

서식 지정함: 글꼴: 기움임꼴

1 [\(CESM2\), *Journal of Advances in Modeling Earth Systems*, 12, e2019MS001882,](#)
2 <https://doi.org/10.1029/2019MS001882>, 2020.

3 [Eskes, J., van Geffen, J., Boersma, F., Eichmann, K. U., Apituley, A., Pedergnana, M.,](#)
4 [Sneep, M., Veeffkind, J. P., and Loyola, D.: Sentinel 5 precursor/TROPOMI Level 2](#)
5 [Product User Manual Nitrogen dioxide, Tech. rep., Report S5P-KNMI-L2-0021-MA,](#)
6 [issue 4.1.0, 11 July 2022, ESA, \[https://sentinel.esa.int/web/sentinel/technical-\]\(https://sentinel.esa.int/web/sentinel/technical-guides/sentinel-5p/products-algorithms\)](#)
7 [guides/sentinel-5p/products-algorithms](#) (last access: 26 February 2024), 2022.

8 Granier, C., Bessagnet, B., Bond, T., D'Angiola, A., van der Gon, H. D., Frost, G. J.,
9 Heil, A., Kaiser, J. W., Kinne, S., Klimont, Z., Kloster, S., Lamarque, J.-F., Liousse,
10 C., Masui, T., Meuleux, F., Mieville, A., Ohara, T., Raut, J.-C., Riahi, K., Schultz, M.
11 G., Smith, S. J., Thompson, A., van Aardenne, J., van der Warf, G. R., and van Vuuren,
12 D. P.: Evolution of anthropogenic and biomass burning emissions of air pollutants at
13 global and regional scales during the 1980 – 2010 period, *Climatic Change*, 109, 163,
14 <https://doi.org/10.1007/s10584-011-0154-1>, 2011.

15 Grell, G. A., Peckham, S. E., Schmitz, R., McKeen, S. A., Frost, G., Shamarock, W. C.,
16 and Eder, B.: Fully coupled “online” chemistry within the WRF model, *Atmos.*
17 *Environ.*, 39, 6957-6975, <https://doi.org/10.1016/j.atmosenv.2005.04.027>, 2005.

18 ~~Heimann, M., Monfray, P., and Polian, G.: Long range transport of Rn 222: A test for~~
19 ~~3D tracer models, *Chem. Geol.*, 70, 98, [https://doi.org/10.1016/0009-](https://doi.org/10.1016/0009-2541(88)90476-7)~~
20 ~~[2541\(88\)90476-7](https://doi.org/10.1016/0009-2541(88)90476-7), 1988.~~

21 Hong, H., Lee, H., Kim, J., Jeong, U., Ryu, J., Lee, D. S.: Investigation of Simultaneous
22 Effects of Aerosol Properties and Aerosol Peak Height on the Air Mass Factors for
23 Space-Borne NO₂ Retrievals, *remote sens.*, 9(3), 208,
24 <https://doi.org/10.3390/rs9030208>, 2017.

25 Huijnen, V., Williams, J., van Weele, M., van Noije, T., Krol, M., Dentener, F., Segers,
26 A., Houweling, S., Peters, W., de Laat, J., Boersma, F., Bergamaschi, P., van

- 1 Velthoven, P., Le Sager, P., Eskes, H., Alkemade, F., Scheele, R., Nédélec, P., and
2 Pätz, H.-W.: The global chemistry transport model TM5: description and evaluation
3 of the tropospheric chemistry version 3.0, *Geosci. Model Dev.*, 3, 445-473,
4 <https://doi.org/10.5194/gmd-3-445-2010>, 2010.
- 5 Jang, Y., Lee, Y., Kim, J., Kim, Y., and Woo, J.-H.: Improvement China point source for
6 improving bottom-up emission inventory, *Asia-Pac. J. Atmos. Sci.*, 56, 107-118,
7 <https://doi.org/10.1007/s13143-019-00115-y>, 2020.
- 8 ~~Kim, H. C., Kim, S., Lee, S. H., Kim, B. U., and Lee, P.: Fine Scale Columnar and~~
9 ~~Surface NO_x concentrations over South Korea: Comparison of Surface Monitors,~~
10 ~~TROPOMI, CMAQ and CAPSS Inventory, *Atmosphere*, 11, 101,~~
11 ~~<https://doi.org/10.3390/atmos11010101>, 2020.~~
- 12 Kim, J., Jeong, U., Ahn, M.-H., Kim, J. H., Park, R. J., Lee, H., Song, C. H., Choi, Y.-
13 S., Lee, K.-J., Yoo, J.-M., Jeong, M.-J., Park, S. K., Lee, K.-M., Song, C.-K., Kim,
14 S.-W., Kim, Y. J., Kim, S.-W., Kim, M., Go, S., Liu, X., Chance, K., Miller, C. C.,
15 Al-Saadi, J., Veihelmann, B., Bhartia, P. K., Torres, O., González Abad, G., Haffner,
16 D. P., Ko, D. H., Lee, S. H., Woo, J.-H., Chong, H., Park, S. S., Nicks, D., Choi, W.
17 J., Moon, K.-J., Cho, A., Yoon, J., Kim, S.-K., Hong, H., Lee, K., Lee, H., Lee, S.,
18 Choi, M., Veekfind, P., Levelt, P. F., Edwards, D. P., Kang, M., Eo, M., Bak, J., Baek,
19 K., Kwon, H.-A., Yang, J., Park, J., Han, K. M., Kim, B.-R., Shin, H.-W., Choi, H.,
20 Lee, E., Chong, J., Cha, Y., Koo, J.-H., Irie, H., Hayashida, S., Kasai, Y., Kanaya, Y.,
21 Liu, C., Lin, J., Crawford, J. H., Carmichael, G. R., Newchurch, M. J., Lefter, B. L.,
22 Herman, J. R., Swap, R. J., Lau, A. K. H., Kurosu, T. P., Jaross, G., Ahlers, B., Dobber,
23 M., McElroy, C. T., and Choi, Y.: New Era of Air Quality Monitoring from Space:
24 Geostationary Environment Monitoring Spectrometer (GEMS), *Bull. Amer. Meteor.*
25 *Soc.*, 101, E1-E22, <https://doi.org/10.1175/BAMS-D-18-0013.1>, 2020.
- 26 Kim, K.-M., Kim, S.-W., Seo, S., Blake, D. R., Cho, S., Crawford, J. H., Emmons, L.
27 K., Fried, A., Herman, J. R., Hong, J., Jung, J., Pfister, G. G., Weinheimer, A. J., Woo,

1 J.-H., and Zhang, Q.: Sensitivity of the WRF-Chem v4.4 simulations of ozone and
2 formaldehyde and their precursors to multiple bottom-up emission inventories over
3 East Asia during the KORUS-AQ 2016 field campaign, *Geosci. Model Dev.*, 17,
4 1931-1955, <https://doi.org/10.5194/gmd-17-1931-2024>, 2024.

5 Kim, S.-W., McDonald, B. C., Brown, S. S., Dube, B., Ferrare, R. A., Frost, G. J., Harley,
6 R. A., Holloway, J. S., Lee, H.-J., McKeen, S. A., Neuman, J. A., Nowak, J. B., Oetjen,
7 H., Ortega, I., Pollack, I. B., Roberts, J. M., Ryerson, T. B., Scarino, A. J., Senff, C.
8 J., Thalman, R., Trainer, M., Volkamer, R., Wagner, N., Washenfelder, R. A., Waxman,
9 E., and Young, C. J.: Modeling the weekly cycle of NO_x and CO emissions and their
10 impacts on O₃ in the Los Angeles-South Coast Air Basin during the CalNex 2010
11 field campaign, *J. Geophys. Res. Atmos.*, 121, 1340-1360,
12 <https://doi.org/10.1002/2015JD024292>, 2016.

13 ~~Kleipool, Q. L., Dobber, M. R., de Haan, J. F., and Levelt, P. F.: Earth surface
14 reflectance climatology from 3 years of OMI data, *J. Geophys. Res. Atmos.*, 113,
15 D18308, <https://doi.org/10.1029/2008JD010290>, 2008.~~

16 ~~Lamsal, L. N., Krotkov, N. A., Vasilkov, A., Marchenko, S., Qin, W., Yang, E. S.,
17 Fasnacht, Z., Joiner, J., Choi, S., Haffner, D., Swartz, W. H., Fisher, B., and Busecela,
18 E.: Ozone Monitoring Instrument (OMI) Aura nitrogen dioxide standard product
19 version 4.0 with improved surface and cloud treatments, *Atmos. Meas. Tech.*, 14,
20 455-479, <https://doi.org/10.5194/amt-14-455-2021>, 2021.~~

21 Lange, K., Richter, Bösch, T., Zilker, B., Latsch, M., Behrens, L. K., Okafor, C. M.,
22 Bösch, H., Burrows, J. P., Merlaud, A., Pinardi, G., Fayt, C., Friedrich, M. M.,
23 Dimitropoulou, E., Van Roozendael, M., Ziegler, S., Ripperger-Lukosiunaite, S.,
24 Kuhn, L., Lauster, B., Wagner, T., Hong, H., Kim, D., Chang, L.-S., Bae, K., Song,
25 C.-K., and Lee, H.: Validation of GEMS tropospheric NO₂ columns and their diurnal
26 variation with ground-based DOAS measurements, *EGUsphere [preprint]*,
27 <https://doi.org/10.5194/egusphere-2024-617>, 2024.

- 1 Levelt, P. F., van den Oord, G. H. J., Dobber, M., R., Mälkki, A., Visser, H., de Vries,
2 J., Stammes, P., Lundell, J. O. V., and Saari, H.: The Ozone Monitoring Instrument,
3 *IEEE Trans. Geosci. Remote Sens.*, 44(5), 1093-1101,
4 <https://doi.org/10.1109/TGRS.2006.872333>, 2006.
- 5 Liu, S., Valks, P. Pinardi, G., Xu, J., Argyrouli, A., Lutz, R., Tilstra, G., Huijnen, V.,
6 Hendric, F., and Van Roozendael, M.: An improved air mass factor calculation for
7 nitrogen dioxide measurements from the Global Ozone Monitoring Experiment-2
8 (GOME-2), *Atmos. Meas. Tech.*, 13, 755-787, [https://doi.org/10.5194/amt-13-755-](https://doi.org/10.5194/amt-13-755-2020)
9 [2020](https://doi.org/10.5194/amt-13-755-2020), 2020.
- 10 Lorente, A., Boersma, K. F., Yu, H., Dörner, S., Hilboll, A., Richter, A., Liu, M., Lamsal,
11 L. N., Barkley, M., De Smedt, I., Van Roozendael, M., Wang, Y., Wagner, T., Beirle,
12 S., Lin, J.-T., Krotkov, N., Stammes, P., Wang, P., Eskes, H. J., and Krol, M.:
13 Structural uncertainty in air mass factor calculation for NO₂ and HCHO satellite
14 retrievals, *Atmos. Mech. Tech.*, 10, 759-782, [https://doi.org/10.5194/amt-10-759-](https://doi.org/10.5194/amt-10-759-2017)
15 [2017](https://doi.org/10.5194/amt-10-759-2017), 2017.
- 16 [Milford, J. B., Russell, A. G., and McRae, G. J.: A new approach to photochemical](https://doi.org/10.1021/es00068a017)
17 [pollution control: implications of spatial patterns in pollutant responses in nitrogen](https://doi.org/10.1021/es00068a017)
18 [oxides and reactive organic gas emissions, *Environ. Sci. Technol.*, 23, 1290-1301,](https://doi.org/10.1021/es00068a017)
19 <https://doi.org/10.1021/es00068a017>, 1989.
- 20 [Munro, R., Lang, R., Klaes, D., Poli, G., Retscher, C., Lindstrot, R., Huckle, R., Lacan,](https://doi.org/10.5194/amt-9-1279-2016)
21 [A., Grzegorski, M., Holdak, A., Kokhanovsky, A., Livschitz, J., and Eisinger, M.:](https://doi.org/10.5194/amt-9-1279-2016)
22 [The GOME-2 instrument on the Metop series of satellites: instrument design,](https://doi.org/10.5194/amt-9-1279-2016)
23 [calibration, and level 1 data processing – an overview, *Atmos. Meas. Tech.*, 9, 1279–](https://doi.org/10.5194/amt-9-1279-2016)
24 [1301, https://doi.org/10.5194/amt-9-1279-2016](https://doi.org/10.5194/amt-9-1279-2016), 2016.
- 25 [Oak, Y. J., Jacob, D. J., Balasus, N., Yang, L. H., Chong, H., Park, J., Lee, H., Lee, G.](https://doi.org/10.5194/amt-9-1279-2016)
26 [T., Ha, E. S., Park, R. J., Kwon, H. A., and Kim, J.: A bias corrected GEMS](https://doi.org/10.5194/amt-9-1279-2016)

서식 지정함: 글꼴: 기움임꼴

1 [geostationary satellite product for nitrogen dioxide using machine learning to enforce](#)
2 [consistency with the TROPOMI satellite instrument, *Atmos. Meas. Tech.*, 17, 5147-](#)
3 [5159, <https://doi.org/10.5194/amt-17-5147-2024>, 2024.](#)

4 Palmer, P. I., Jacob, D. J., Chance, K., Martin, R. V., Spurr, R. J. D., Kurosu, T. P., Bey,
5 I., Yantosca, R., Fiore, A., and Li, Q.: Air mass factor formulation for spectroscopic
6 measurements from satellites: Application to formaldehyde retrievals from the
7 Global Ozone Monitoring Experiment, *J. Geophys. Res.*, 106, 14539-14550,
8 <https://doi.org/10.1029/2000JD900772>, 2001.

9 ~~Richter, A. and Burrows, J. P., 2002: Tropospheric NO₂ from GOME Measurements~~,
10 ~~*Advances in Space Research*, Volume: 29 Issue: 11 Pages: 1673-1683 Published:~~
11 ~~2002 ———— DOI10.1016/S0273-1177(02)00123-0, 1673-1683,~~
12 ~~[https://doi.org/10.1016/S0273-1177\(02\)00100-X](https://doi.org/10.1016/S0273-1177(02)00100-X), 2002.~~

서식 지정함: 아래 첨자

서식 지정함: 글꼴: 기움임꼴

13 Richter, A., Lange, K., Burrows, J. Bösch, J., Kim, S.-W., Seo, S., Kim, K.-M., Hong,
14 H., Lee, H., and Park, J.: An improved tropospheric NO₂ retrieval for GEMS, *Atmos.*
15 *Meas. Tech.*, in preparation, 2024.

16 Rozanov, V. V., Rozanov, A. V., Kokhanovsky, A. A. and Burrows, J. P.: Radiative
17 transfer through terrestrial atmosphere and ocean: Software package SCIATRAN, *J.*
18 *Quant. Spectrosc. Radiat. Transf.*, 133, 13-71,
19 <https://doi.org/10.1016/j.jqsrt.2013.07.004>, 2014.

20 ~~Shah, V., Jacob, D. J., Li, K., Silvern, R. F., Zhai, S., Liu, M., Lin, J., and Zhang, Q.:~~
21 ~~Effect of changing NO_x lifetime on the seasonality and long-term trends of satellite-~~
22 ~~observed tropospheric NO₂ columns over China, *Atmos. Chem. Phys.*, 20, 1483-1495,~~
23 ~~<https://doi.org/10.5194/acp-20-1483-2020>, 2020.~~

24 Skamarock, W. C., Klemp, J. B., Dudhia, J., Gill, D. O., Liu, Z., Berner, J., Wang, W.,
25 Powers, J. G., Duda, M. G., Barker, D. M., Huang, X.-Y.: A Description of the
26 Advanced Research WRF Model Version 4 (No. NCAR/TN-556+STR),

- 1 <https://doi.org/10.5065/1dfh-6p97>, 2021.
- 2 Tilstra, L. G., de Graaf, M., Trees, V. J. H., Litvinov, P., Dubovik, O., and Stammes, P.:
3 A directional surface reflectance climatology determined from TROPOMI
4 observations, *Atmos. Meas. Tech.*, 17, 2235-2256, [https://doi.org/10.5194/amt-17-](https://doi.org/10.5194/amt-17-2235-2024)
5 [2235-2024](https://doi.org/10.5194/amt-17-2235-2024), 2024.
- 6 ~~van Geffen, J., Eskes, H., Compernelle, S., Pinardi, G., Verhoelst, T., Lambert, J.-C.,
7 Sneep, M., ter Linden, M., Ludewig, A., Boersma, K. F., and Veeffkind, J. P.: Sentinel~~
8 ~~5PTROPOMINO2 retrieval: impact of version v2.2 improvements and comparisons~~
9 ~~with OMI and ground-based data, *Atmos. Meas. Tech.*, 15, 2037-2060,~~
10 ~~<https://doi.org/10.5194/amt-15-2037-2022>, 2022.~~
- 11 Veeffkind, J. P., Aben, I., McMullan, K., Förster, H., de Vries, J., Otter, G., Claas, J.,
12 Eskes, H. J., de Haan, J. F., Kleipool, Q., van Weele, M., Hasekamp, O., Hoogeveen,
13 R., Landgraf, J., Snel, R., Tol, P., Ingmann, P., Voors, R., Kruizinga, B., Vink, R.,
14 Visser, H., and Levelt, P. F.: TROPOMI on the ESA Sentinel-5 Precursor: A GMES
15 mission for global observations of the atmospheric composition for climate, air
16 quality and ozone layer applications, *Remote Sens. Environ.*, 120, 70-83,
17 <https://doi.org/10.1016/j.rse.2011.09.027>, 2012.
- 18 ~~Valin, L. C., Russell, A. R., Hudman, R. C., and Cohen, R. C.: Effects of model~~
19 ~~resolution on the interpretation of satellite NO₂ observations, *Atmos. Chem. Phys.*,~~
20 ~~11, 11647-11655, <https://doi.org/10.5194/11-11647-2011>, 2011.~~
- 21 ~~Vlemmixx, T., Hendrick, F., Pinardi, G., De Smedt, I., Fayt, C., Hermans, C., Pitters, A.,~~
22 ~~Wang, P., Levelt, P., and Van Roozendael, M.: MAX-DOAS observations of aerosols,~~
23 ~~formaldehyde and nitrogen dioxide in the Beijing area: comparison of two profile~~
24 ~~retrieval approaches, *Atmos. Meas. Tech.*, 8, 941-963, [https://doi.org/10.5194/amt-8-](https://doi.org/10.5194/amt-8-941-2015)~~
25 ~~[941-2015](https://doi.org/10.5194/amt-8-941-2015), 2015.~~
- 26 Williams, J. E., Boersma, K. F., Le Sager, P., and Verstraeten, W. W.: The high-

1 resolution version of TM5-MP for optimized satellite retrievals: description and
2 validation, *Geosci. Model Dev.*, 10, 721–750, [https://doi.org/10.5194/gmd-10-721-](https://doi.org/10.5194/gmd-10-721-2017)
3 [2017](https://doi.org/10.5194/gmd-10-721-2017), 2017.

4 Woo, J.-H., Choi, K.-C., Kim, H. K., Baek, B. H., Jang, M., Eum, J.-H., Song, C. H.,
5 Ma, Y.-I., Sunwoo, Y., Chang, L.-S., and Yoo, S. H.: Development of an
6 anthropogenic emissions processing system for Asia using SMOKE, *Atmos. Environ.*,
7 58, 5-13, <https://doi.org/10.1016/j.atmosenv.2011.10.042>, 2012.

8 wrf-model: WRF, Github [code], <https://github.com/wrf-model/WRF/release/tag/v4.4>,
9 last access: 18 May 2022.

10 [Yang, L. H., Jacob, D. J., Colombi, N. K., Zhai, S., Bates, K. H., Shah, V., Beaudry, E.,
11 Yantosca, R. M., Lin, H., Brewer, J. F., Chong, H., Travis, K. R., Crawford, J. H.,
12 Lamsal, L. N., Koo, J. H., and Kim, J.: Tropospheric NO₂ vertical profiles over South
13 Korea and their relation to oxidant chemistry: implications for geostationary satellite
14 retrievals and the observations of NO₂ diurnal variation from space, *Atmos. Chem.
15 Phys.*, 23, 2465–2481, <https://doi.org/10.5194/acp-23-2465-2023>, 2023.](https://doi.org/10.5194/acp-23-2465-2023)

16 Yang, L. H., Jacob, D. J., Dang, R., Oak, Y. J., Lin, H., Kim, J., Zhai, S., Colombi, N.
17 K., Pendergrass, D. C., Beaudry, E., Shah, V., Feng, X., Yantosca, R. M., Chong, H.,
18 Park, J., Lee, H., Lee, W.-J., Kim, S., Kim, E., Travis, K. R., Crawford, J. H., Liao,
19 H., Interpreting GEMS geostationary satellite observations of the diurnal variation
20 of nitrogen dioxide (NO₂) over East Asia, *Atmos. Chem. Phys.*,
21 <https://doi.org/10.5194/acp-24-7027-2024>, 2024.

22

1 **List of Tables**

2 [Table 1. Description of the experimental designs. MACCity provides hourly-constant](#)
3 [emissions, while the others provide hourly-varying emissions.](#) ~~Table 1. Description of~~
4 ~~the experiment designs.~~

5

1 **List of Figures**

2 **Figure 1.** Diurnal variabilities of normalized NO_x emissions for CTRL (black) and
3 TM5 (gray) cases over the SMA region.

4 **Figure 2.** Diurnal behavior patterns of retrieved (solid) and *a priori* (dashed) NO₂
5 TropVCDs during weekdays in (a) January, (b) April, (c) July, and (d) October 2021
6 over the SMA region. Gray lines identify the TM5 case, while black lines
7 represent the CTRL case. The pixels with wind speed faster than 3m/s are
8 excluded.

9 Figure 3. Spatial distributions of air mass factor (AMF) differences (CTRL – TM5) in
10 January, April, July, and October 2021. The pixels with wind speed faster than 3m/s are
11 excluded.

12 Figure 4. Diurnal patterns of the air mass factor during weekdays in (a) January, (b)
13 April, (c) July, and (d) October 2021 over the SMA region. Gray lines indicate the TM5
14 run, while black lines mean the CTRL run. The pixels with wind speed faster than 3m/s
15 are excluded.

16 Figure 5. Vertical profiles of *a priori* NO₂ mixing ratios at 08, 10, 12, 14, and 16 LT
17 from the TM5 (gray) and CTRL (black) runs in January, April, July, and October 2021
18 over the SMA region.

19 Figure 6. Diurnal patterns of retrieved (solid) and *a priori* (dashed) NO₂ TropVCDs in
20 July 2021 over SMA region from the CTRL run (black) and (a) CONST run (red), (b)
21 FINE run (pink), and (c) MIXED run (yellow). The pixels with wind speed faster than
22 3m/s are excluded. Note that diurnal changes of *a priori* NO₂ TropVCDs in the CONST
23 run occur during calculating domain-averaged values – the location and number of
24 pixels excluded during the collocation with satellite data vary over time during the day.

25 Figure 7. Vertical profiles of *a priori* NO₂ mixing ratios at 08, 10, 12, 14, and 16 LT
26 from the CTRL (black), CONST (red), FINE (pink), and MIXED run (yellow) in

1 January, April, July, and October 2021 over the SMA region.

2

3 **Figure 83.** Diurnal patterns of boundary layer mean OH concentrations over the SMA
4 region in January (black), April (yellow), July (red), and October (blue) 2021 from the
5 CTRL ~~casrun~~.

6 **Figure 94.** Spatial distributions of retrieved NO₂ TropVCDs in January, April, July, and
7 October 2021 taking the a priori data for the AMF form the TM5 run. The scenes with
8 wind speed faster than 3m/s are excluded to minimize the impact of rapid
9 transport. ~~Spatial distributions of retrieved NO₂ TropVCDs in January, April, July, and~~
10 ~~October 2021 from the TM5 casrun. The pixels with wind speed faster than 3m/s are~~
11 ~~excluded.~~

12 **Figure 105.** Same as Figure 9, except that a priori values for the AMF calculation are
13 taken from the CTRL run. ~~Same as Figure 4, except from the CTRL casrun.~~

14 **Figure 116.** Similar to Figure 9, but for the differences of NO₂ TropVCD between
15 CTRL and TM5 run (CTRL – TM5). ~~Same as Figure 4, except for the differences~~
16 ~~between CTRL and TM5 casrun (CTRL – TM5).~~

17 **Figure 12.** Diurnal patterns of retrieved NO₂ TropVCDs from the CTRL run in (a)
18 January, (b) April, (c) July, and (d) October 2021 over the SMA region. Black lines
19 indicate the NO₂ TropVCD values with wind-filtered data; only the scenes with wind
20 speed lower than 3m/s are utilized. Blue lines are the averaged values without any wind
21 filters. The green line is for case of strong-wind run with the NO₂ TropVCD being
22 selected and averaged for wind speeds faster than 5m/s in January.

23 **Figure 127.** Diurnal patterns of retrieved NO₂ TropVCDs from the CTRL casrun in (a)
24 January, (b) April, (c) July, and (d) October 2021 over the SMA region. Black lines
25 indicate the VCD values with wind-filtered data; only the pixels with wind speed lower
26 than 3m/s are utilized. Blue lines are the averaged values without any wind filters. A

메모 포함[JP5]: Where are the green lines I do not see any green lines in April July and October ???

1 ~~green line is for the strong wind case~~~~run~~ ~~the data with wind speed faster than 5m/s~~
2 ~~are selected to average.~~

3 ~~**Figure 8.** Spatial distributions of air mass factor (AMF) differences (CTRL—TM5) in~~
4 ~~January, April, July, and October 2021. The pixels with wind speed faster than 3m/s are~~
5 ~~excluded.~~

6 ~~**Figure 9.** Diurnal patterns of the air mass factor during weekdays in (a) January, (b)~~
7 ~~April, (c) July, and (d) October 2021 over the SMA region. Gray lines indicate the TM5~~
8 ~~case, while black lines mean the CTRL case. The pixels with wind speed faster than~~
9 ~~3m/s are excluded.~~

10 ~~**Figure 10.** Vertical profiles of *a priori* NO₂ mixing ratios at 08, 10, 12, 14, and 16 LT~~
11 ~~from the TM5 (gray) and CTRL (black) cases in January, April, July, and October 2021~~
12 ~~over the SMA region.~~

13 ~~**Figure 11.** Diurnal patterns of retrieved (solid) and *a priori* (dashed) NO₂-TropVCDs~~
14 ~~in July 2021 over SMA region from the CTRL case (black) and (a) CONST case (red),~~
15 ~~(b) FINE case (pink), and (c) MIXED case (yellow). The pixels with wind speed faster~~
16 ~~than 3m/s are excluded. Note that diurnal changes of *a priori* NO₂-TropVCDs in the~~
17 ~~CONST case occur during calculating domain averaged values—the location and~~
18 ~~number of pixels excluded during the collocation with satellite data vary over time~~
19 ~~during the day.~~

20 ~~**Figure 12.** Vertical profiles of *a priori* NO₂ mixing ratios at 08, 10, 12, 14, and 16 LT~~
21 ~~from the CTRL (black), CONST (red), FINE (pink), and MIXED case (yellow) in~~
22 ~~January, April, July, and October 2021 over the SMA region.~~

23

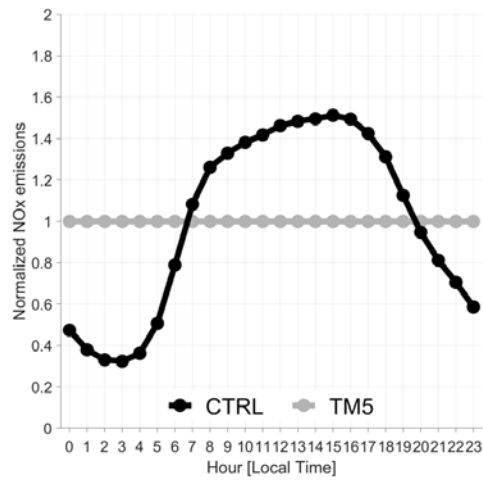
1 **Table 1.** Description of the experimental designs. MACCity provides hourly-constant
 2 emissions, while the others provide hourly-varying emissions.

CaseRun name	Model	Horizontal resolution	Emission inventory
TM5	TM5	1° × 1°	MACCity
CTRL		28 × 28 km ²	2021AQNEA
CONST ^{a)}	WRF-Chem v4.4	28 × 28 km ²	2021AQNEA
FINE		12 × 12 km ²	2021AQNEA
MIXED		28 × 28 km ²	(VOC) KORUSv5 (others) 2021AQNEA

3

4 ^{a)} CONST caserun uses hourly-varying emission inventory, but only data of 13:45 LT
 5 were utilized to compute AMF.

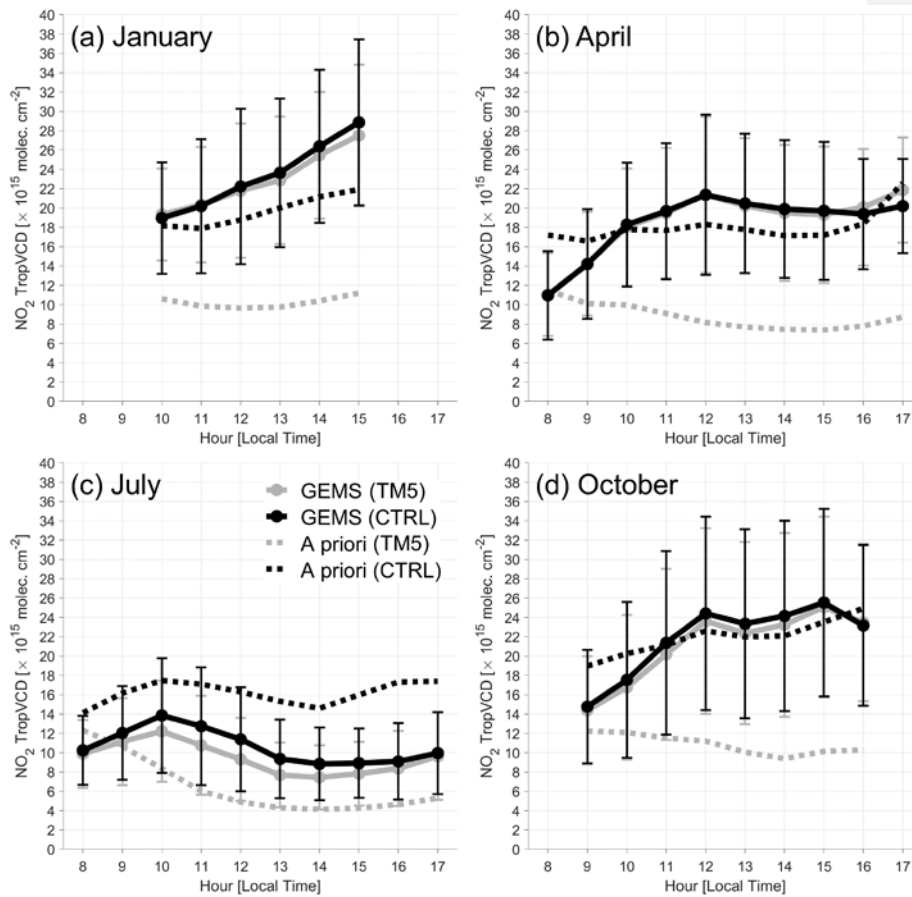
6



1

2 **Figure 1.** Diurnal variabilities of normalized NO_x emissions for CTRL (black) and

3 TM5 (gray) easeruns over the SMA region.

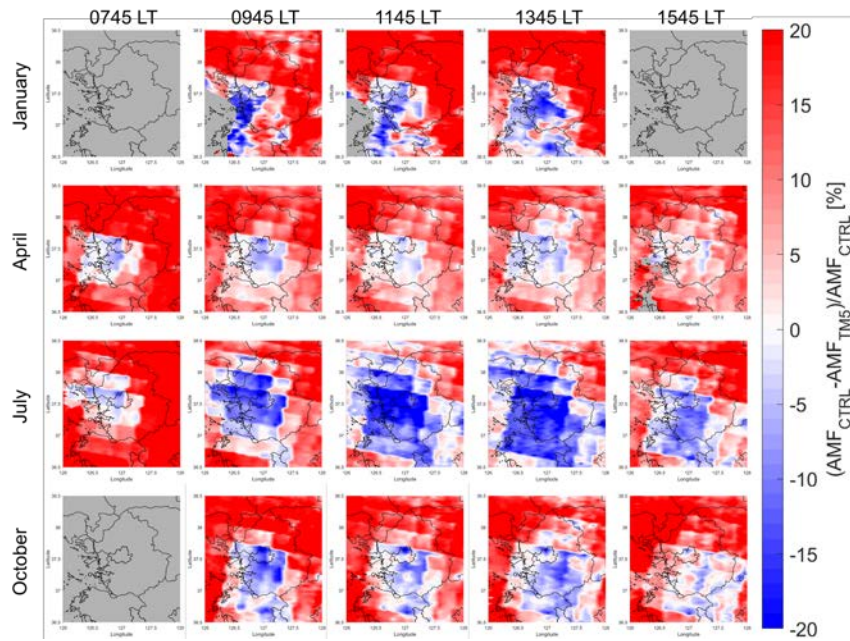


1

2 **Figure 2.** [Diurnal behavior of retrieved \(solid\) and *a priori* \(dashed\) NO₂ TropVCDs](#)
 3 [during weekdays in \(a\) January, \(b\) April, \(c\) July, and \(d\) October 2021 over the SMA](#)
 4 [region. Gray lines identify the TM5 run, while black lines represent the CTRL run. The](#)
 5 [pixels with wind speed faster than 3m/s are excluded.](#) [Diurnal patterns of retrieved \(solid\)](#)
 6 [and *a priori* \(dashed\) NO₂ TropVCDs during weekdays in \(a\) January, \(b\) April, \(c\)](#)
 7 [July, and \(d\) October 2021 over the SMA region. Gray lines indicate the TM5 caserun,](#)
 8 [while black lines mean the CTRL caserun.](#) [The pixels with wind speed faster than 3m/s](#)
 9 [are excluded.](#)

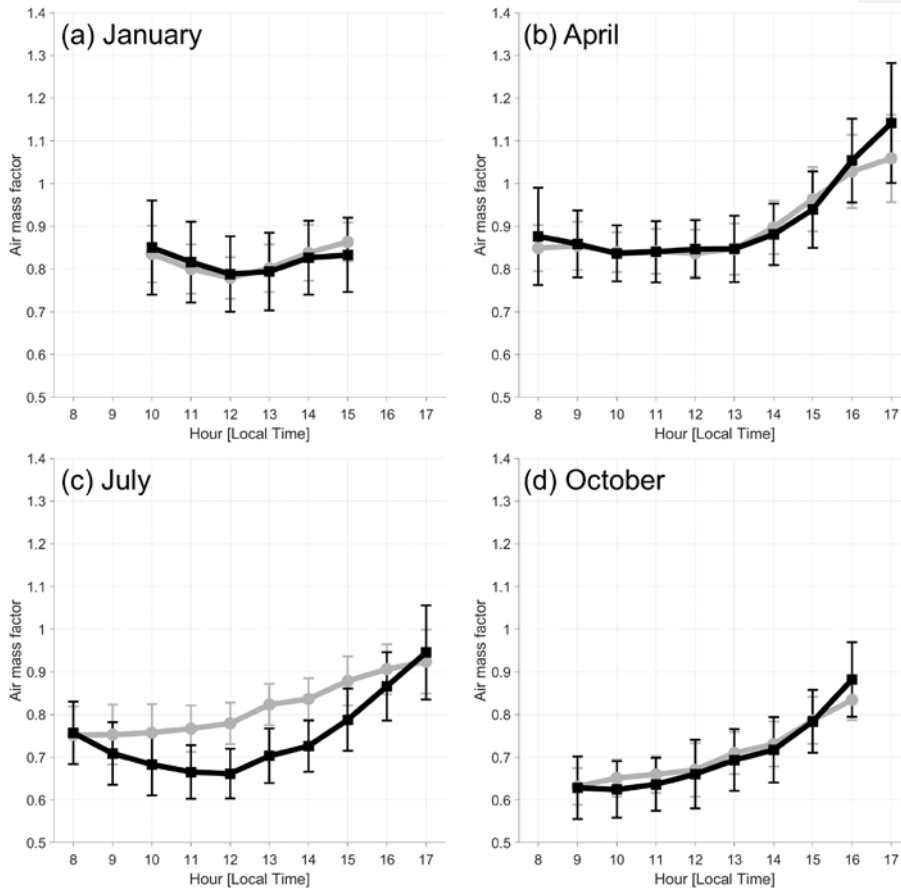
10

1



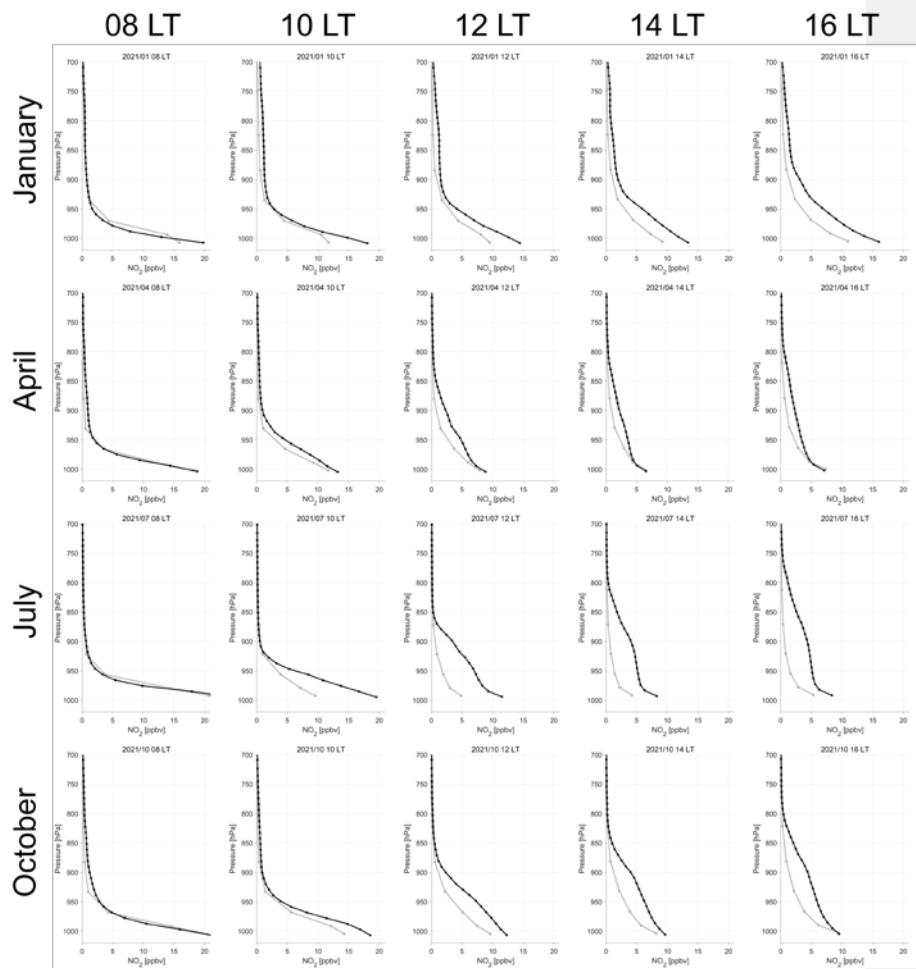
2

3 **Figure 3.** Spatial distributions of air mass factor (AMF) differences (CTRL – TM5) in
4 January, April, July, and October 2021. The pixels with wind speed faster than 3m/s are
5 excluded.



1
2 **Figure 4.** Diurnal patterns of the air mass factor during weekdays in (a) January, (b)
3 April, (c) July, and (d) October 2021 over the SMA region. Gray lines indicate the TM5
4 run, while black lines mean the CTRL run. The pixels with wind speed faster than 3m/s
5 are excluded.

6 _____



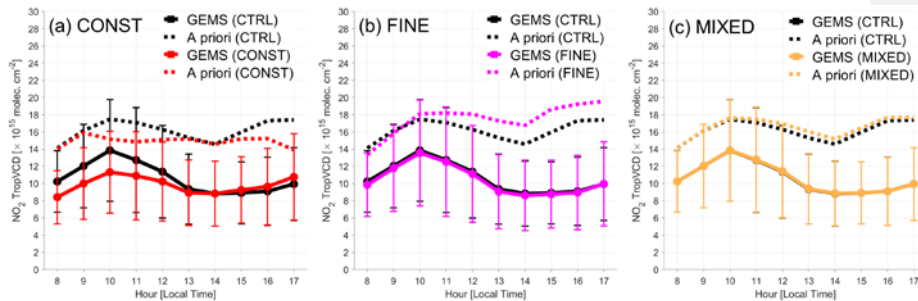
1

2 **Figure 5.** Vertical profiles of *a priori* NO₂ mixing ratios at 08, 10, 12, 14, and 16 LT

3 from the TM5 (gray) and CTRL (black) runs in January, April, July, and October 2021

4 over the SMA region.

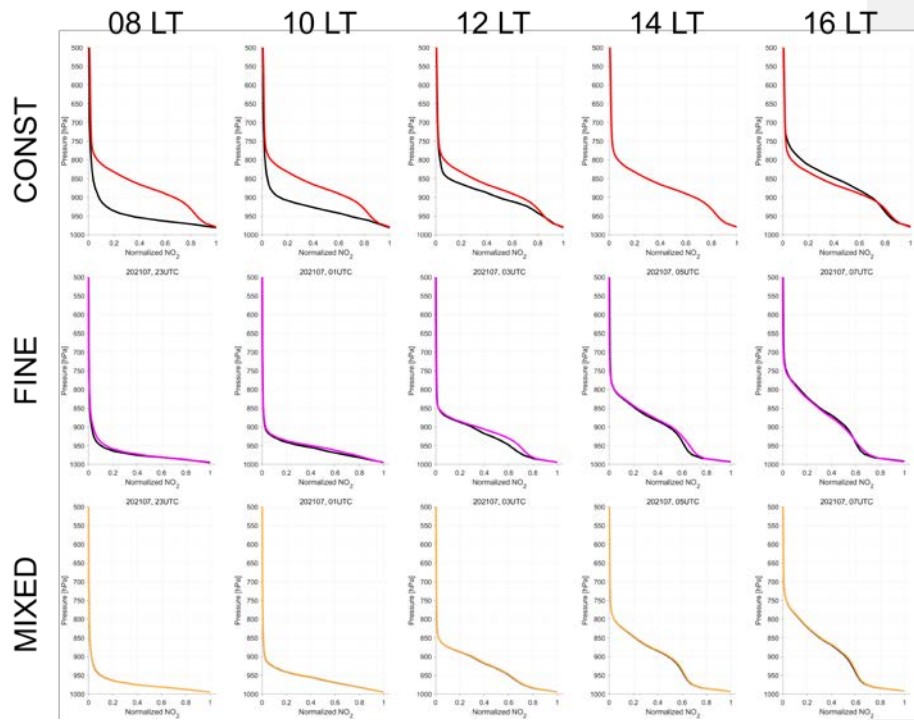
5 _____



1

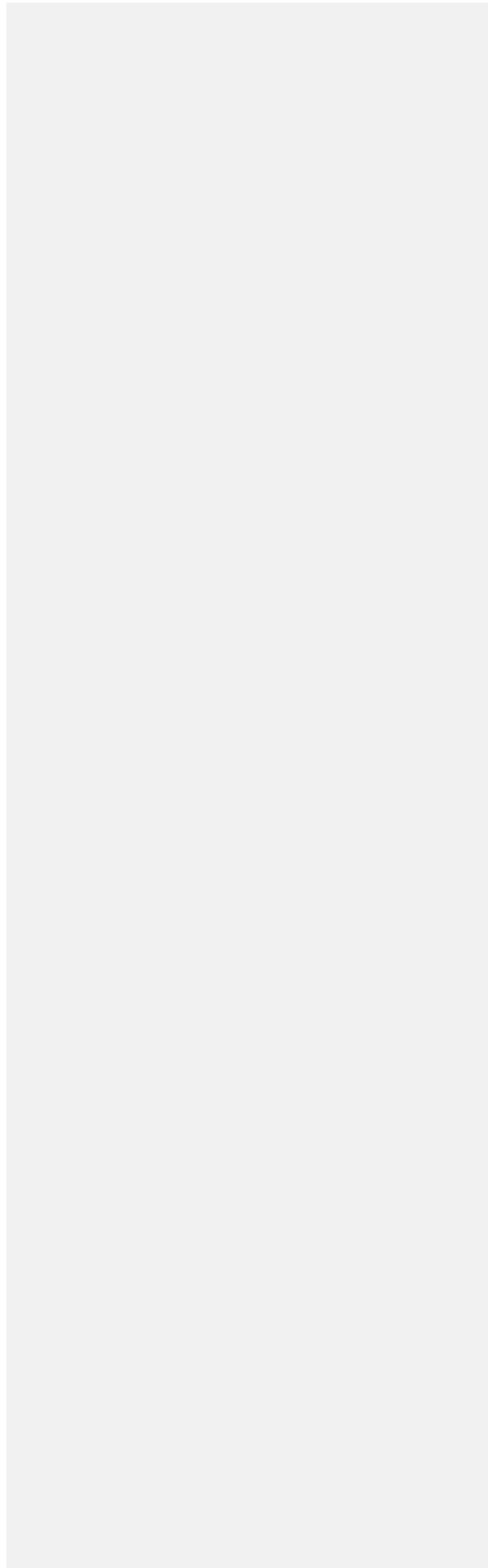
2 **Figure 6.** Diurnal patterns of retrieved (solid) and *a priori* (dashed) NO₂ TropVCDs in
 3 July 2021 over SMA region from the CTRL run (black) and (a) CONST run (red), (b)
 4 FINE run (pink), and (c) MIXED run (yellow). The pixels with wind speed faster than
 5 3m/s are excluded. Note that diurnal changes of *a priori* NO₂ TropVCDs in the CONST
 6 run occur during calculating domain-averaged values – the location and number of
 7 pixels excluded during the collocation with satellite data vary over time during the day.

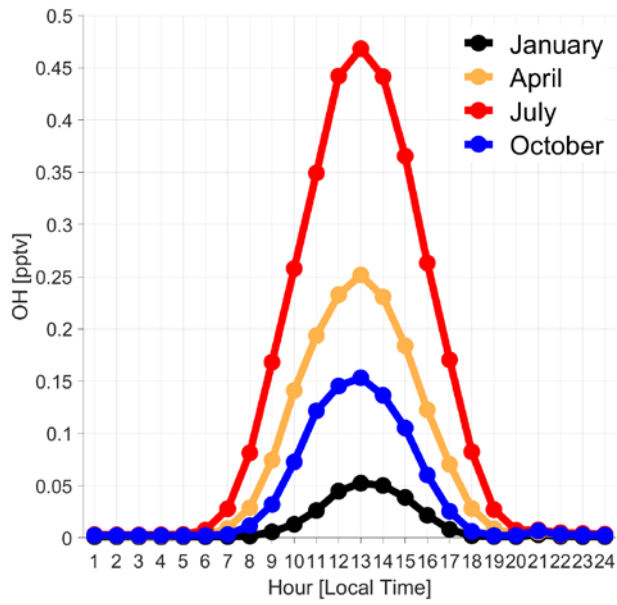
8



1
2 **Figure 7.** Vertical profiles of *a priori* NO₂ mixing ratios at 08, 10, 12, 14, and 16 LT
3 from the CTRL (black), CONST (red), FINE (pink), and MIXED run (yellow) in
4 January, April, July, and October 2021 over the SMA region.

5 서식 있음: 단락의 첫 줄이나 마지막 줄 분리 허용,
6 한글과 영어 간격을 자동으로 조절하지 않음, 한글과
7 숫자 간격을 자동으로 조절하지 않음

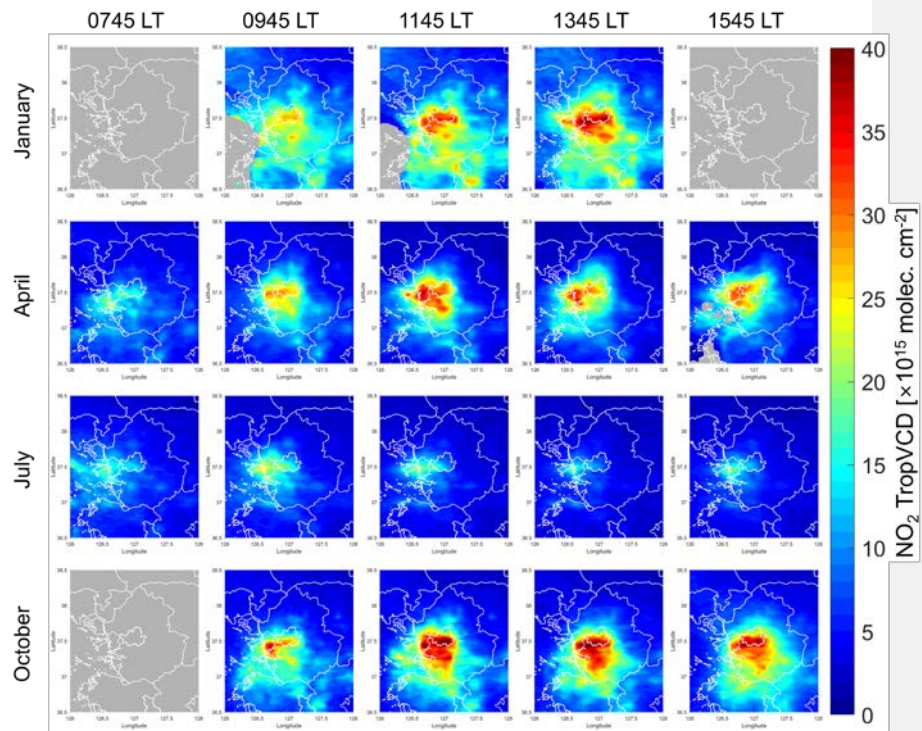




1

2 **Figure 83.** Diurnal patterns of boundary layer mean OH concentrations over the SMA
 3 region in January (black), April (yellow), July (red), and October (blue) 2021 from the
 4 CTRL [easerun](#).

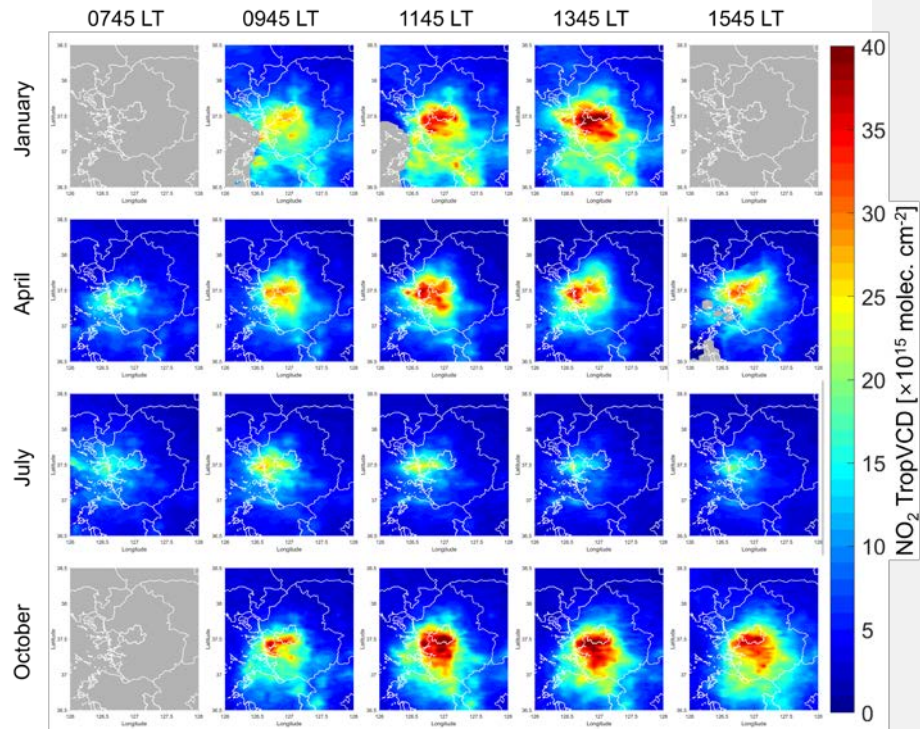
5



1

2 **Figure 94.** Spatial distributions of retrieved NO₂ TropVCDs in January, April, July, and
 3 October 2021 taking the a priori data for the AMF from the ~~from the~~ TM5 ~~case~~run. The
 4 scenepixels with wind speed faster than 3m/s are excluded to minimize the impact of
 5 rapid transport.-

6

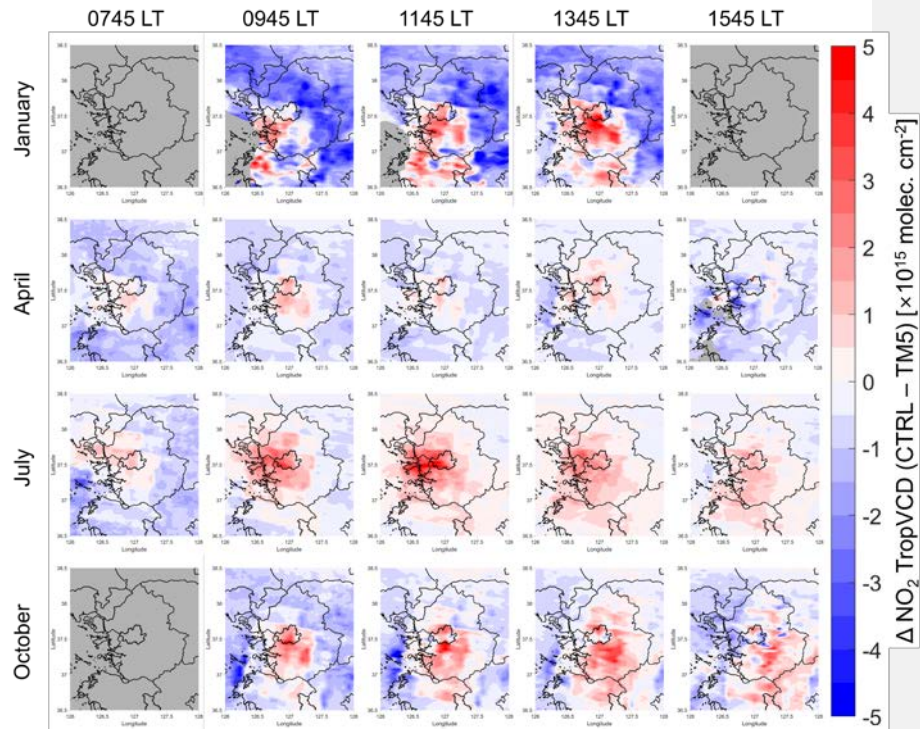


1

2 **Figure 105.** Same as Figure 94, except that *a priori* values for the AMF calculation are
 3 taken from the CTRL *eserun*.

서식 지정함: 글꼴: 기움임꼴

4

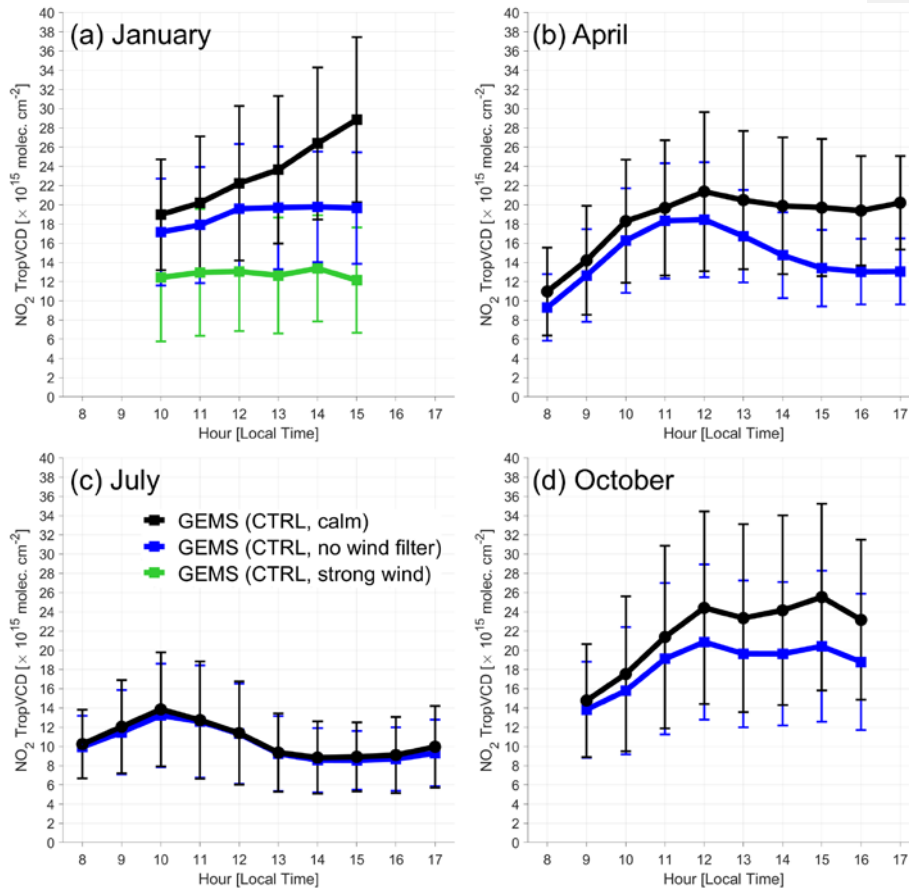


1

2 **Figure 116.** Similar to ~~figure Same as~~ Figure 894, but for the ~~except for the~~ differences
 3 of NO_2 TropVCD between CTRL and TM5 ~~easerun~~ (CTRL - TM5).

서식 지정함: 아래 첨자

4



1

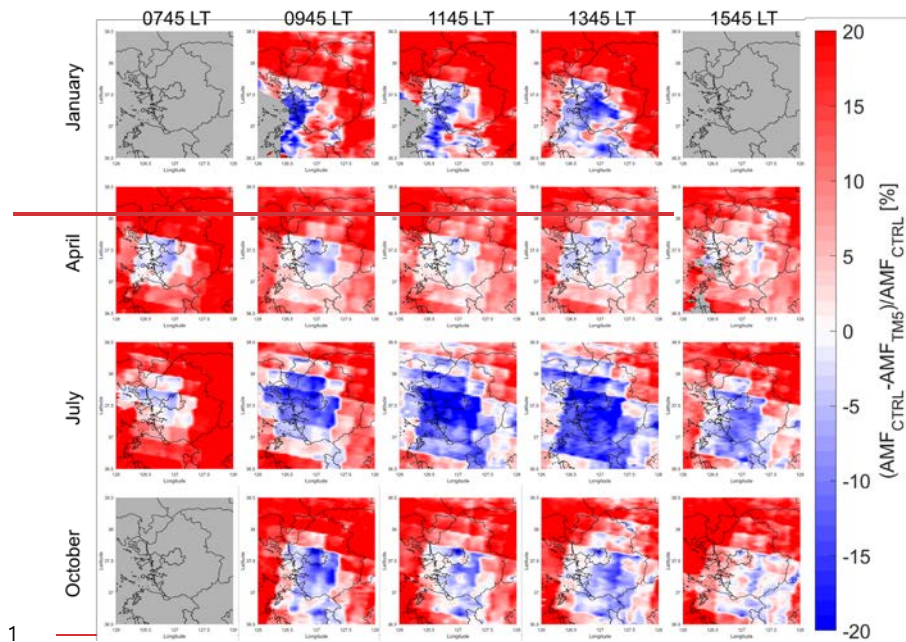
2 **Figure 127.** Diurnal patterns of retrieved NO₂ TropVCDs from the CTRL easerun in (a)
 3 January, (b) April, (c) July, and (d) October 2021 over the SMA region. Black lines
 4 indicate the NO₂ Trop-VCD values with wind-filtered data; only the scenespixels with
 5 wind speed lower than 3m/s are utilized. Blue lines are the averaged values without any
 6 wind filters. TheA green lines are-is for case of-is for the strong-wind easerun with -
 7 the NO₂ TropVCD-data being selected and averaged forwith wind speeds faster than
 8 5m/s in January-are selected to average.

메모 포함[JP6]: Where are the green lines I do not see any green lines in April July and October ???

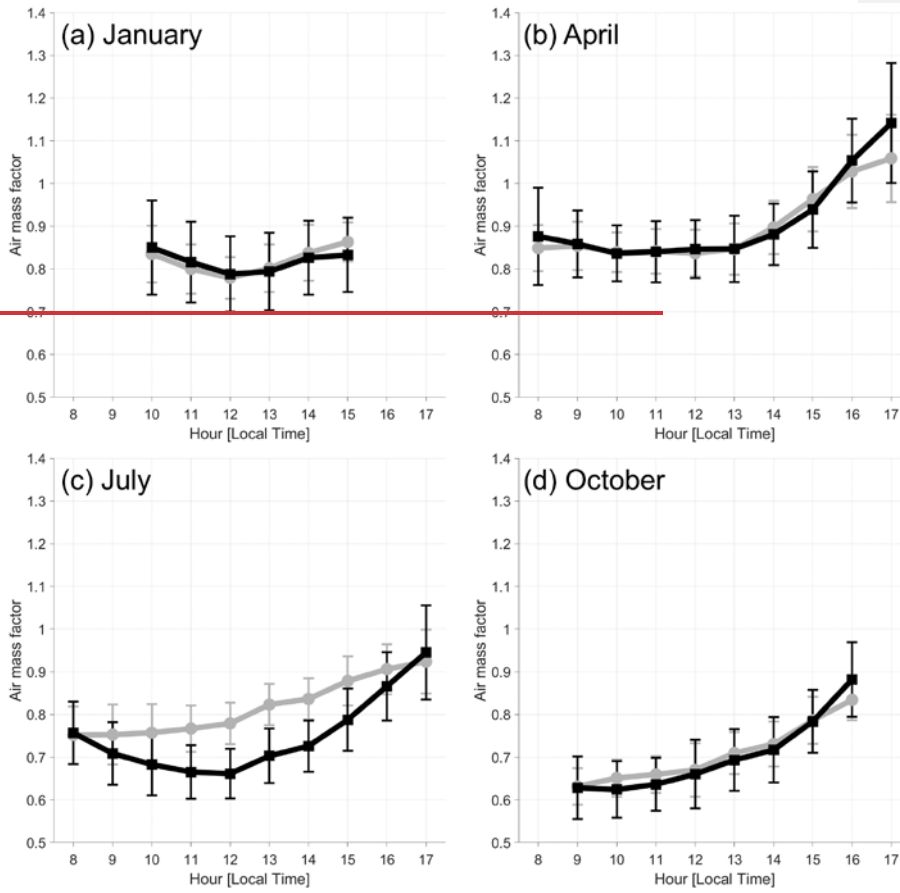
서식 지정함: 아래 첨자

서식 지정함: 아래 첨자

9



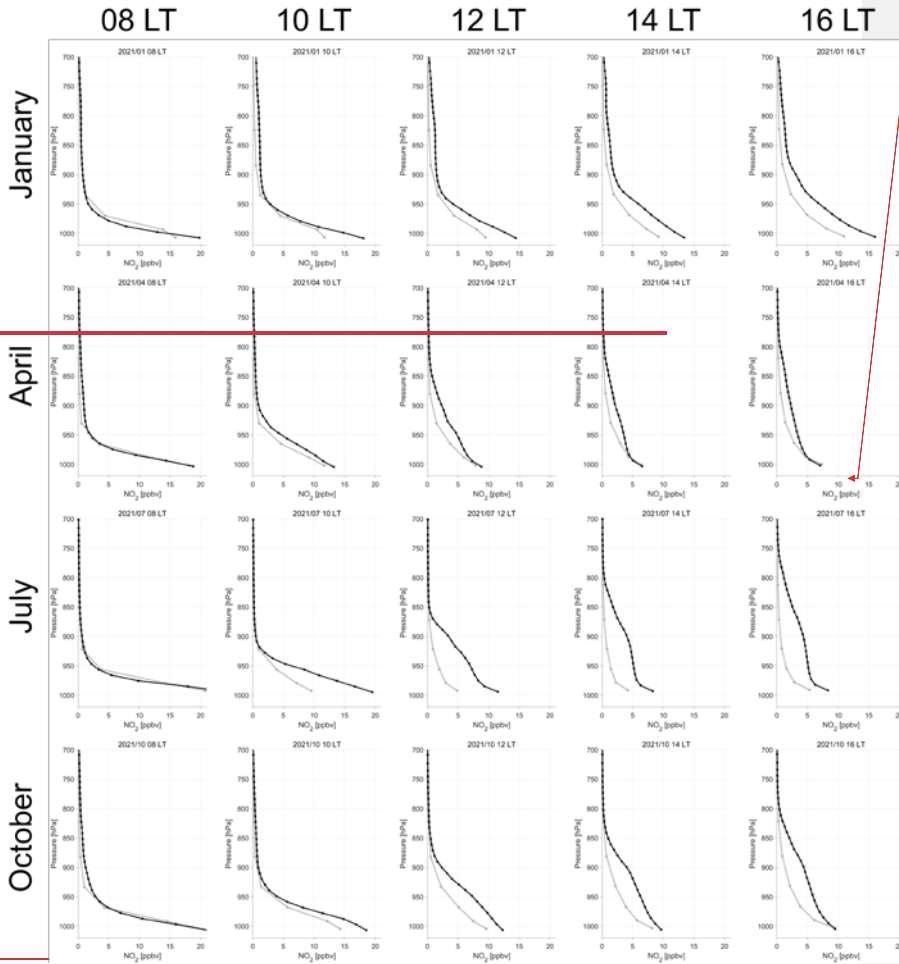
1
 2 **Figure 8.** Spatial distributions of air mass factor (AMF) differences (CTRL—TM5) in
 3 January, April, July, and October 2021. The pixels with wind speed faster than 3m/s are
 4 excluded.



1

2 **Figure 9.** Diurnal patterns of the air mass factor during weekdays in (a) January, (b)
 3 April, (c) July, and (d) October 2021 over the SMA region. Gray lines indicate the TMS
 4 case, while black lines mean the CTRL case. The pixels with wind speed faster than
 5 3m/s are excluded.

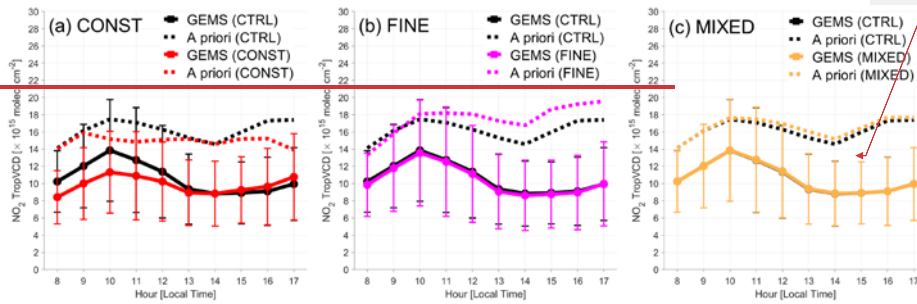
6



서식 있음: 단락의 첫 줄이나 마지막 줄 분리 방지, 한글과 영어 간격을 자동으로 조절, 한글과 숫자 간격을 자동으로 조절

1
2 **Figure 10.** Vertical profiles of *a priori* NO₂ mixing ratios at 08, 10, 12, 14, and 16 LT
3 from the TMS (gray) and CTRL (black) cases in January, April, July, and October 2021
4 over the SMA region.

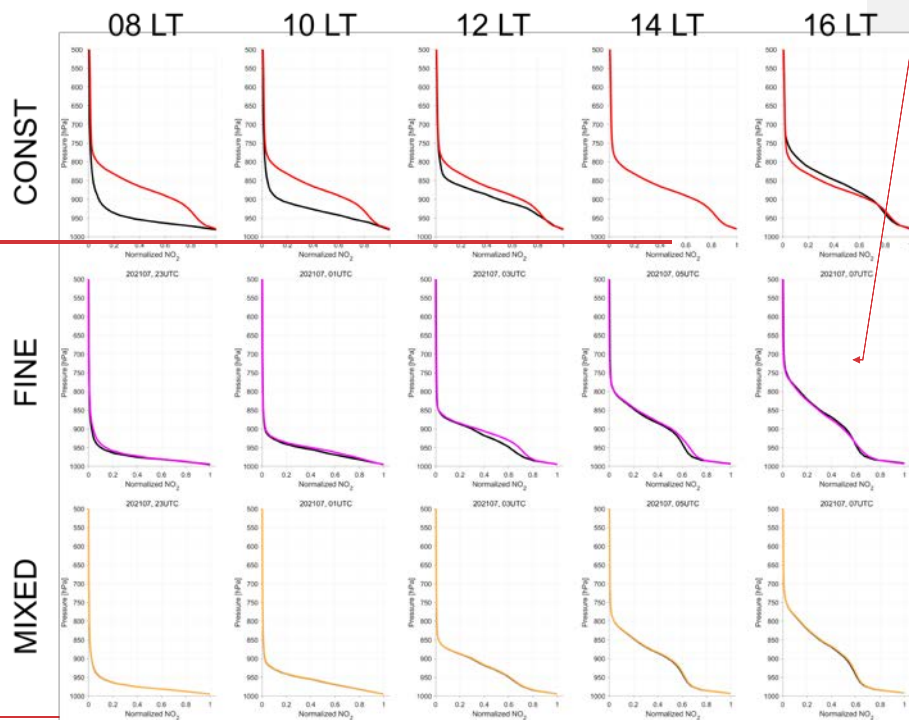
5 _____



서식 있음: 단락의 첫 줄이나 마지막 줄 분리 방지, 한글과 영어 간격을 자동으로 조절, 한글과 숫자 간격을 자동으로 조절

1
2
3
4
5
6
7
8
9

Figure 11. Diurnal patterns of retrieved (solid) and *a priori* (dashed) NO_2 -TropVCDs in July 2021 over SMA region from the CTRL case (black) and (a) CONST case (red), (b) FINE case (pink), and (c) MIXED case (yellow). The pixels with wind speed faster than 3m/s are excluded. Note that diurnal changes of *a priori* NO_2 -TropVCDs in the CONST case occur during calculating domain-averaged values—the location and number of pixels excluded during the collocation with satellite data vary over time during the day.



서식 있음: 단락의 첫 줄이나 마지막 줄 분리 방지,
한글과 영어 간격을 자동으로 조절, 한글과 숫자 간격을
자동으로 조절

1
2 **Figure 12.** Vertical profiles of *a priori* NO₂ mixing ratios at 08, 10, 12, 14, and 16 LT
3 from the CTRL (black), CONST (red), FINE (pink), and MIXED case (yellow) in
4 January, April, July, and October 2021 over the SMA region.

5